Science of the Total Environment 912 (2024) 168999

Contents lists available at ScienceDirect

Science of the Total Environment

journal homepage: www.elsevier.com/locate/scitotenv

Comparison between mechanical and hydrological reinforcement effects of cultivated plants on shallow slope stability

Massimiliano Bordoni [a,*], Valerio Vivaldi [a], Alessia Giarola [a], Roberto Valentino [b], Marco Bittelli [c], Claudia Meisina [a]

[a] Department of Earth and Environmental Sciences, University of Pavia, Via Ferrata 1, 27100 Pavia, Italy
[b] Department of Chemistry, Life Sciences and Environmental Sustainability, University of Parma, Parco Area delle Scienze 157/A, 43124 Parma, Italy
[c] Department of Agricultural Sciences, University of Bologna, Viale Fanin 44, 40127 Bologna, Italy

HIGHLIGHTS

- Multidisciplinary study of root reinforcement effects of different agroecosystems
- Different land uses have effects on soil hydrological trends.
- Land use influences both mechanical and hydrological root reinforcements.
- Root hydrological reinforcement 1–2 times higher than mechanical one in summer
- Hydrological reinforcement of grapevines similar to mechanical one in wet periods

GRAPHICAL ABSTRACT

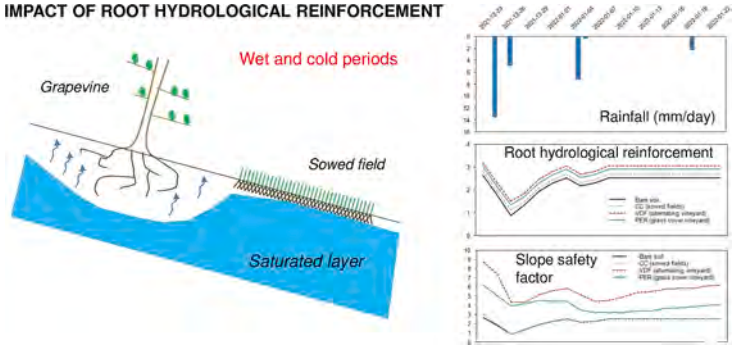

ARTICLE INFO

Editor: Manuel Esteban Lucas-Borja

Keywords:
Root reinforcement
Land management
Shallow landslides
Soil hydrology

ABSTRACT

Root reinforcement, provided by plants in soil, can be exerted by a mechanical effect, increasing soil shear strength for the presence of roots, or by a hydrological effect, induced by plant transpiration. No comparisons have been still carried out between mechanical and hydrological reinforcements on shallow slope stability in typical agroecosystems. This paper aims to compare these effects induced by sowed fields and vineyards and to assess their effects towards the shallow slope staibility. Root mechanical reinforcement has been assessed through Root Bundle Model-Weibull. Root hydrological reinforcement has been evaluated using an empirical relationship with monitored or modelled pore water pressure. Each reinforcement has been inserted in a stability model to quantify their impacts on susceptibility towards shallow landslides. Considering the same environment, corresponding to a typical agroecosystem of northern Italian Apennines, land use has significant effects on saturation degree and pore water pressure, influencing hydrological reinforcement. Root hydrological reinforcement effect is higher in summer, although rainfall-induced shallow landslides rarely occur in this period due to dry soil conditions. Instead, in wet and cold periods, when shallow landslides can develop more frequently, the stabilizing contribution of mechanical reinforcement is on average higher than the hydrological reinforcement. In vineyards, the hydrological reinforcement effect could be observed also during autumn, winter and spring periods, giving a contribution to slope stability also in these conditions. This situation occurs when plants uptake

* Corresponding author.
E-mail address: massimiliano.bordoni01@universitadipavia.it (M. Bordoni).

https://doi.org/10.1016/j.scitotenv.2023.168999
Received 20 June 2023; Received in revised form 28 November 2023; Accepted 28 November 2023
Available online 29 November 2023

enough water from soil to reduce significantly pore water pressure, guaranteeing values of hydrological reinforcement of 1–3 kPa at 1 m from ground, in agreement with measured mechanical root reinforcement (up to 1.6 kPa). These results suggest that both hydrological and mechanical effects of vegetation deserve high regard in susceptibility towards shallow landslides, helping in selection of the best land uses to reduce probability of occurrence of these failures over large territories.

1. Introduction

Sloping terrains located in hilly and mountainous regions around the world have undergone extensive modifications to promote the cultivation of plants and grasses for food production. These modifications include both maintaining the natural slopes and implementing various forms of tillage and other alterations to make the land more suitable for agriculture (Tarolli and Straffelini, 2020; Tarolli et al., 2021). In Europe, >20 % of sloping terrains are either cultivated or designated for agricultural use (Panagos et al., 2021). In Asia, Africa, and the Americas, 10–47 % of sloping lands are deemed suitable for croplands, and there has been a consistent expansion of approximately 2–8 million hectares from 2003 to 2019 (Potapov et al., 2022).

However, the geological-geomorphological features of cultivated hillslopes, exacerbated by unsuitable local agricultural practices and land management, contribute to an inherent susceptibility of these terrains to slope instabilities, particularly involving the shallowest soil layers. These instabilities manifest as rainfall-induced soil erosion and shallow landslides (Lesschen et al., 2008; Froude and Petley, 2018). Moreover, the heightened intensity of rainfall events driven by climate change (IPCC, 2022) is leading to an increased likelihood of shallow slope instabilities, with direct consequences for local economies, landscapes, soil fertility, and biodiversity (Tarolli, 2018).

Slope instabilities affecting cultivated hillslopes can be mitigated through various structural and non-structural stabilization and remediation measures. These measures aim to either reduce the destabilizing forces acting along a hillslope or enhance the shear strength properties of the slope soils (de Jesus Arce-Mojica et al., 2019). Typical structural interventions such as land levelling, retaining walls, piles, gabions, and shallow and subsurface drainage systems can yield immediate positive effects on slope stabilization without requiring an extended establishment period. However, they can be costly and are often applicable only at a site-specific scale, potentially impacting the landscape and environmental continuity (Moos et al., 2018).

Bioengineering techniques, which leverage the mechanical and hydrological benefits of vegetation to enhance soil shear strength, can also be implemented at catchment or larger scales. However, they may be constrained by the depth to which plant root systems penetrate, and a transition period of up to several decades may be necessary to observe positive effects on slope stabilization (Cammeraat et al., 2005). Furthermore, although plant activity and biomass can contribute to increased soil organic content and nutrient levels, these techniques have the potential to compromise the cultural heritage, landscape features, and biodiversity of a region, with associated impacts on socio-economic development (Arnaez et al., 2011).

For these reasons, specific cultivated crops and agricultural practices could serve as effective means to mitigate shallow slope instabilities without altering the landscapes, environment, and economic characteristics of traditional rural areas (Gariano et al., 2018; Bordoni et al., 2020). Therefore, it becomes essential to assess the feasibility of traditionally cultivated plant species as tools for safeguarding or reducing the susceptibility of sloping terrain to shallow slope failures, comparing them to different types of cultivated crops.

Like other plants, including shrubs and grasses (Morgan and Rickson, 2003; Wu, 2012; Cohen and Schwarz, 2017), cultivated crops can contribute to slope stability through various mechanisms, which can also act in combination (Bordoloi and Ng, 2020; Ng et al., 2022). Vegetation's soil reinforcement primarily arises from the mechanical reinforcement provided by the small and flexible roots within the soil matrix (Schmidt et al., 2001; Bischetti et al., 2009; Schwarz et al., 2013; Stokes et al., 2014; Masi et al., 2021; Mao, 2022), as well as a "hydrological reinforcement effect". The "hydrological reinforcement effect" involves an increase in soil strength resulting from a reduction in water content and corresponding pore water pressure due to plant transpiration (Veylon et al., 2015; Gonzalez-Ollauri and Mickovski, 2017; Yildiz et al., 2019; Ni et al., 2018, 2019; Ng et al., 2020; Boldrin et al., 2018, 2021; Capobianco et al., 2021; Chen et al., 2021; Liu et al., 2021). Additionally, other processes such as rainfall interception (Gonzalez-Ollauri and Mickovski, 2017), concentrated stem flow (Levia and Germer, 2015), subsurface preferential flows through root channels (Vergani and Graf, 2016; Leung et al., 2018), and modification of soil hydrological properties by roots (Lu et al., 2020; Zhu et al., 2022) can further influence soil hydrology and consequently impact the stability of slopes.

Several studies have been conducted to quantify the mechanical root reinforcement offered by various cultivated plants and grasses in continental and Mediterranean climates. These include grapevines, cardoons, and various types of grasses used for feed production (Bordoni et al., 2016, 2019, 2020; Rossi et al., 2022). However, a comprehensive assessment of the hydrological effects induced by specific cultivated vegetation on shallow slope stability has not yet been undertaken, especially when compared to the quantified soil reinforcement provided by the same vegetation types from a mechanical perspective.

This analysis holds particular significance in hilly and mountainous regions where agriculture plays a pivotal role in the local economy. The Italian Apennines, an orogenic mountain chain stretching across the entire Italian Peninsula, serve as a notable example. The land use distribution in this region reflects the profound human influence on the environment and the strong agricultural orientation of the territory. In the highest mountain ranges, woodlands coexist with extensive cultivated lands and pastures (Brambilla et al., 2010), while the low-lying hilly areas are dedicated to viticulture and olive cultivation (Raggi et al., 2015). The geological and geomorphological characteristics of the Italian Apennines make the cultivated sloping areas highly susceptible to rainfall-induced shallow landslides. This susceptibility is evident from numerous triggering events that have occurred in various sectors or catchments throughout the Italian Apennines in recent years (Montrasio and Valentino, 2008; Giannecchini et al., 2012; Cevasco et al., 2014; Grelle et al., 2014; Ciurleo et al., 2016; Salciarini et al., 2017; Bordoni et al., 2019).

However, certain aspects require more in-depth investigation to assess and compare the mechanical and hydrological reinforcement effects of cultivated plants in regions susceptible to rainfall-induced shallow slope instabilities. These aspects can be summarized as follows:

- Long-term monitoring under various meteorological conditions was conducted to assess the hydrological effects induced in soil by different cultivated vegetation. This will enable quantification of the extent of the hydrological reinforcement effect induced by different plants and its variability across different periods.
- Evaluating and comparing the impact of both mechanical and hydrological reinforcement effects provided by the same type of cultivated plant on susceptibility to rainfall-induced shallow slope failures. This analysis aims to determine whether these two processes offer similar levels of soil reinforcement or if there are significant differences.

- Developing models to understand the triggering mechanisms of shallow landslides and assess whether the mechanical and hydrological effects induced by different cultivated plants can enhance slope stability, even during highly critical rainfall events.

With these questions in mind, this paper aims to assess and compare the mechanical and hydrological reinforcement effects induced by various types of cultivated plants to quantify their impact on shallow slope stability. Specifically, the primary objectives of this paper are as follows: i) To compare the mechanical reinforcement of soil provided by different cultivated plants; ii) To monitor the soil's hydrological responses on slopes cultivated with various plant types, quantifying the differing effects of hydrological reinforcement and their variations over time; iii) To evaluate and compare the influence of mechanical and hydrological reinforcement effects, both provided by the same type of cultivated plant, on susceptibility to rainfall-induced shallow landslides; and iv) To determine whether the mechanical and hydrological reinforcement effects offered by different cultivated plants can enhance or hinder slope stability during events that have the potential to trigger shallow landslides.

The test sites were situated in a characteristic setting within the northern Italian Apennines, specifically in the hilly sector of Oltrepò Pavese (Fig. 1). This region is emblematic of the typical geological, geomorphological, environmental, and land use characteristics found throughout the Italian Apennines.

2. Materials and methods

2.1. The test-sites

The hilly area of Oltrepò Pavese in northwestern Italy (Fig. 1a) marks the northwestern extremity of the Italian Apennines, covering approximately 1000 km2. The elevation of the slopes in this region varies from 50 to 600 m above sea level (m a.s.l.), and the slope angles range from 5 to 45°. Oltrepò Pavese experiences a temperate/mesothermal climate, as per Köppen's classification of world climates, characterized by an average annual temperature of 13 °C and an annual rainfall of 694 mm.

Autumn receives the highest rainfall, contributing to 32 % of the total annual precipitation, with the peak occurring in November when cumulative rainfall reaches 112 mm. Additionally, both winter and spring months each account for approximately 25 % of the annual rainfall. In contrast, summer is the least rainy season, contributing only 18 % of the total annual rainfall, with just 38 mm of rainfall recorded in July.

The bedrock lithology in this area varies (Fig. 1b). In the northern part, there is a Mio-Pliocenic succession comprised of arenaceous, conglomeratic, marly, and evaporitic deposits. The hillslopes in this region are very steep, typically with slope angles exceeding 20°. They are covered with superficial soils resulting from the weathering of the bedrock, and these soils exhibit sandy silts or clayey-sandy silts textures with thicknesses ranging from a few centimetres to 2.5 m.

Moving to the central part of the area, we find Cretaceous flysch formations and other Eocenic-Miocenic marls, calcareous marls, sandstones, and scaly shales as the primary lithological bedrocks. Slopes here have typical inclinations of 5–20° and are characterized by silty clays and clays with silts, with thicknesses ranging from 1.0 to 4.0 m. This region also experiences deep, slow-moving landslides.

In the southern part, Mesozoic flysch formations and melanges with a block-in-matrix texture are prevalent. Hillslopes in this area are generally less steep, with slopes ranging from 5 to 15°. The predominant soils in this region are characterized by a silty clay texture and have thicknesses exceeding 1.0–2.0 m.

The land use in this region is characterized by various agroecosystems interspersed with areas covered by natural vegetation, as noted by Bordoni et al. in 2020. >39 % of the area is enveloped by woodlands dominated by broadleaf species such as black locust, Norway maple, European hackberry, buckthorn, European hophornbeam, and flowering plants.

Around 15 % of the study area consists of shrubs and grasses, primarily composed of hemicryptophytes and chamaephytes, which are prevalent on the uncultivated slopes. Approximately 30 % of the study area comprises active agroecosystems, primarily vineyards (22 %) and

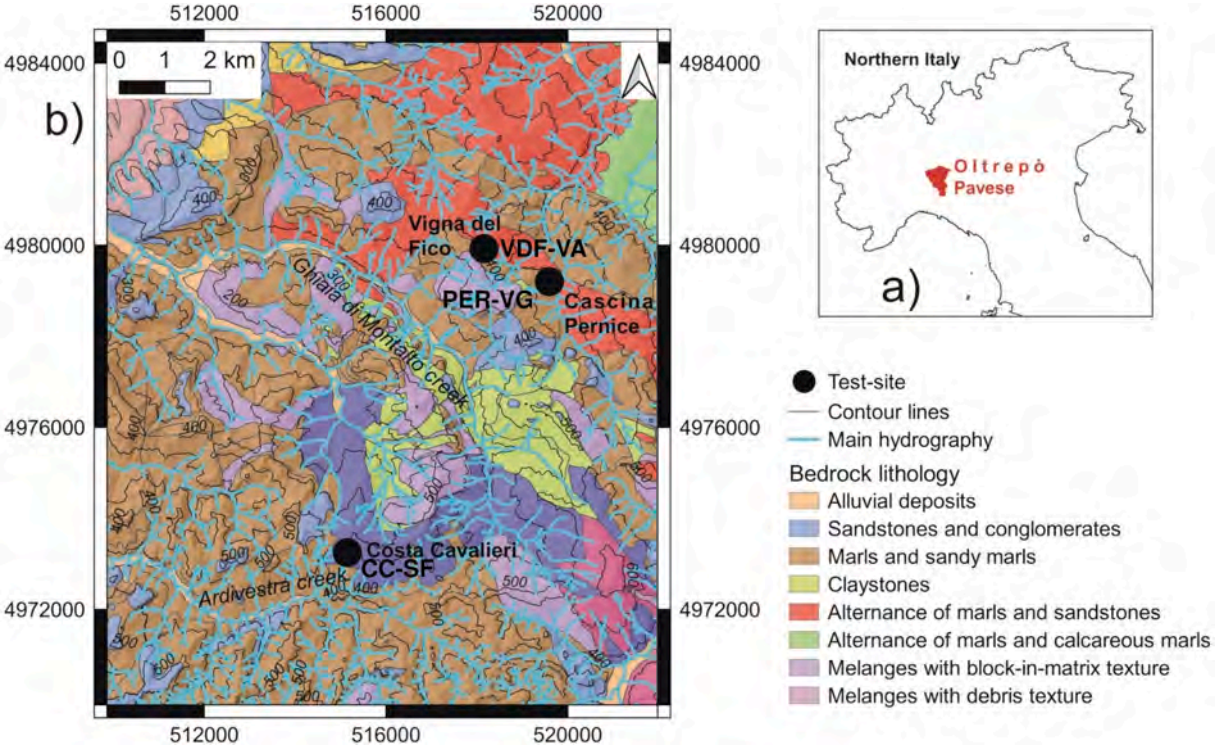

Fig. 1. Test-sites location (a) and their main geological and geomorphological settings (b).

cultivated fields (8 %), with crops like alfalfa and wheat being the predominant choices for cultivation.

Oltrepò Pavese is highly susceptible to shallow landslides triggered by intense rainfall events. According to Bordoni et al. (2020), approximately 1.7 % of the study area, equivalent to 8.1 km2, has been affected by >2500 shallow landslides since 2009. Most of these slope instabilities initially manifest as shallow rotational-translational failures, eventually evolving into earthflows, as described by Cruden and Varnes (1996). These landslides typically measure between 10 and 70 m in width and 10 to 500 m in length, with sliding surfaces typically found at depths of approximately 1 m from the ground level, regardless of the land use where these slope failures occur.

Of these shallow landslides, 46 % affected cultivated slopes, 25 % occurred in sowed fields, and 21 % took place in vineyards, as reported by Bordoni et al. (2020). Furthermore,the majority of triggering events occurred during the wettest periods of the year, notably in the spring, autumn, and winter months, with a particular concentration between March and May and between October and December. The rainfall events responsible for triggering these landslides typically had durations ranging from 4 to 105 h and cumulated precipitation amounts spanning from 30 to 134 mm, as detailed in Bordoni et al'.s findings from 2020.

Three test-sites were carefully chosen and monitored within the Oltrepò Pavese area to assess the mechanical and hydrological reinforcement effects on the occurrence of shallow slope instabilities. These test-sites shared similar geological and geomorphological characteristics, making them suitable for comparative analysis. However, they each represented different agroecosystems, allowing us to emphasize the distinctions among various cultivated plants.

The Costa Cavalieri test-site (CC-SF) was situated in central Oltrepò Pavese (Fig. 1b) and served as a representative example of a sowed field where alfalfa and wheat were cultivated alternately. Alfalfa and wheat have been grown in this test site for over 40 years, including the 7-year monitoring period analyzed in this study. Agricultural activities primarily affected the top 0.2–0.3 m of soil, involving tillage of the shallowest soil layer before planting the vegetation.

The Cascina Pernice (PER-VG) and Vigna del Fico (VDF-VA) test-sites were also located in central Oltrepò Pavese, northwest of the Costa Cavalieri test-site (Fig. 1b). These sites represented sloping vineyards with different interrow management practices. In PER-VG, a permanent grass coverwas maintained in the interrows. In contrast, VDF-VA employed alternating tillage and grass cover management, involving tillage in every second interrow while leaving the other rows uncultivated and covered with natural grass. This alternating practice was carried out annually in September–October, with tillage performed in the previously untouched interrows and the previously tilled interrows maintained under grass cover. Both of these practices were consistently followed for >10 years in both test-sites (13 years in PER-VG and 12 years in VDF-VA).

In both vineyards, the chosen cultivar is the Pinot Noir grape variety, with rows spaced approximately 2.4–2.5 m apart and the individual plants within the same row spaced at around 0.8–0.9 m from each other.

In terms of geomorphology (Fig. 2, Table 1), all the selected test-sites were situated at medium slope elevations ranging from 250 to 510 m a.s.l. They were positioned on south-facing hillslopes with moderate steepness, typically ranging from 7 to 18°. Notably, CC-SF exhibited a high susceptibility to shallow landslides, as evidenced by incidents recorded in 2009, 2014, and 2020 (Fig. 2a and Table 1).

Both CC-SF and VDF-VA experienced deep, slow-moving landslides, characterized as roto-translational landslides that evolved into flows with sliding surfaces situated at depths exceeding 4 m from ground level. However, these landslides have remained inactive in recent years. On the other hand, PER-VG and VDF-VA were not impacted by shallow slope failures (Fig. 2b and c, Table 1).

The physical and hydrological characteristics of the soils in the test-sites exhibited significant similarities (Fig. 3, Table 2).

At CC-SF, the soils were silty clay and originated from the weathering of bedrock, specifically melanges with a block-in-matrix texture. From the ground surface down to approximately 0.9 m, the upper soil (US) layer exhibited a silty clay texture with high plasticity and a notable carbonate content in the form of soft concretions. The unit weight of this layer ranged from 18.6 to 19.0 kN/m3.Below this layer, between depths of 0.9 to 1.4 m, there was a calcic soil layer (CAL) with a texture and plasticity similar to the upper layer but with a higher unit weight, approximately 20.3 kN/m3 and a greater carbonate content of 26.7 %. In the CAL layer, carbonate concretions were notably compact, varying in size from centimetres to decimeters. Saturated hydraulic conductivity decreased with depth, with the US layer having the highest value, approximately 10^{-5} m/s, while the CAL layer exhibited a saturated hydraulic conductivity lower than that of the US layer, at around 10^{-6} m/s.

At PER-VG and VDF-VA, the soils resulted from the weathering of marls and arenaceous marls. Similar to CC-SF, the US (US) layer in both of these vineyards exhibited silty clay or clayey silt textures, high plasticity, and a notable carbonate content in the form of soft concretions. The unit weight of this layer ranged from 18.1 to 20.1 kN/m^3. The thickness of this layer was similar in both vineyards, measuring 0.5 m in PER-VG and 0.6 m in VDF-VA, slightly less than that of CC-SF. Beneath the US layer, a CAL layer was still present in both PER-VG and VDF-VA, extending to depths of 1.2 and 1.3 m from ground level, respectively. The CAL layer in these vineyards featured a clayey silt texture in PER-VG and a silty clay texture in VDF-VA, with medium-high plasticity, high unit weight (ranging from 20.3 to 21.0 kN/m^3), and a significant abundance of compact millimetric to centimetric carbonate concretions, accounting for 21.0 % in PER-VG and 36.0 % in VDF-VA. Similar to CC-SF, a decrease in saturated hydraulic conductivity was observed. US layers had values ranging from $8.8{\cdot}10^{-5}$ to $2.3{\cdot}10^{-6}$ m/s, which were approximately two times higher than the values measured in the CAL layers, ranging from $3.2{\cdot}10^{-5}$ to $1.0{\cdot}10^{-6}$ m/s.

As previously demonstrated by Bordoni et al. (2019), different vegetation types and soil management practices have a significant impact on the saturated hydraulic conductivity values in test-sites with similar textural and physical properties. Specifically, the VDF-VA site, characterized by alternating management of vineyard interrows, exhibited higher values for this parameter compared to the other sites, consistent with similar experimental measurements conducted in various land management scenarios in the Oltrepò Pavese area (Bordoni et al., 2019).

2.2. Root mechanical reinforcement

Root Bundle Model - Weibull (RBMw; Schwarz et al., 2013) was employed to calculate the mechanical reinforcement of roots (denoted as c_r) at each testsite. In addition to considering various stages of increasing load and root failure occurring at forces smaller than the applied load, this model incorporated a strain step-loading fibre bundle model. This model was capable of accounting for both the mechanical and geometrical properties of the roots, as well as the complete distribution of roots along the depth and their maximum resisting force (Schwarz et al., 2013).

As per the RBMw model, the required root mechanical properties included the parameters describing the power-law relationships between root diameters and tensile force at rupture, specifically Young's modulus and root length, respectively. These parameters were measured for the analyzed land uses and are documented in Table 3 of Bordoni et al. (2019, 2020). The mechanical properties of the root system were then integrated with the root system architecture throughout the soil depth, which was estimated based on the number of roots found along a soil profile. The quantification of roots was accomplished using the root-wall technique (Bohm, 1979). In the CC-SF area, all identified roots belonged to the planted crops, which characterized this specific test-site. However, in the PER-VG and VDF-VA areas, grapevine roots were measured and distinguished from any spontaneous grass roots that

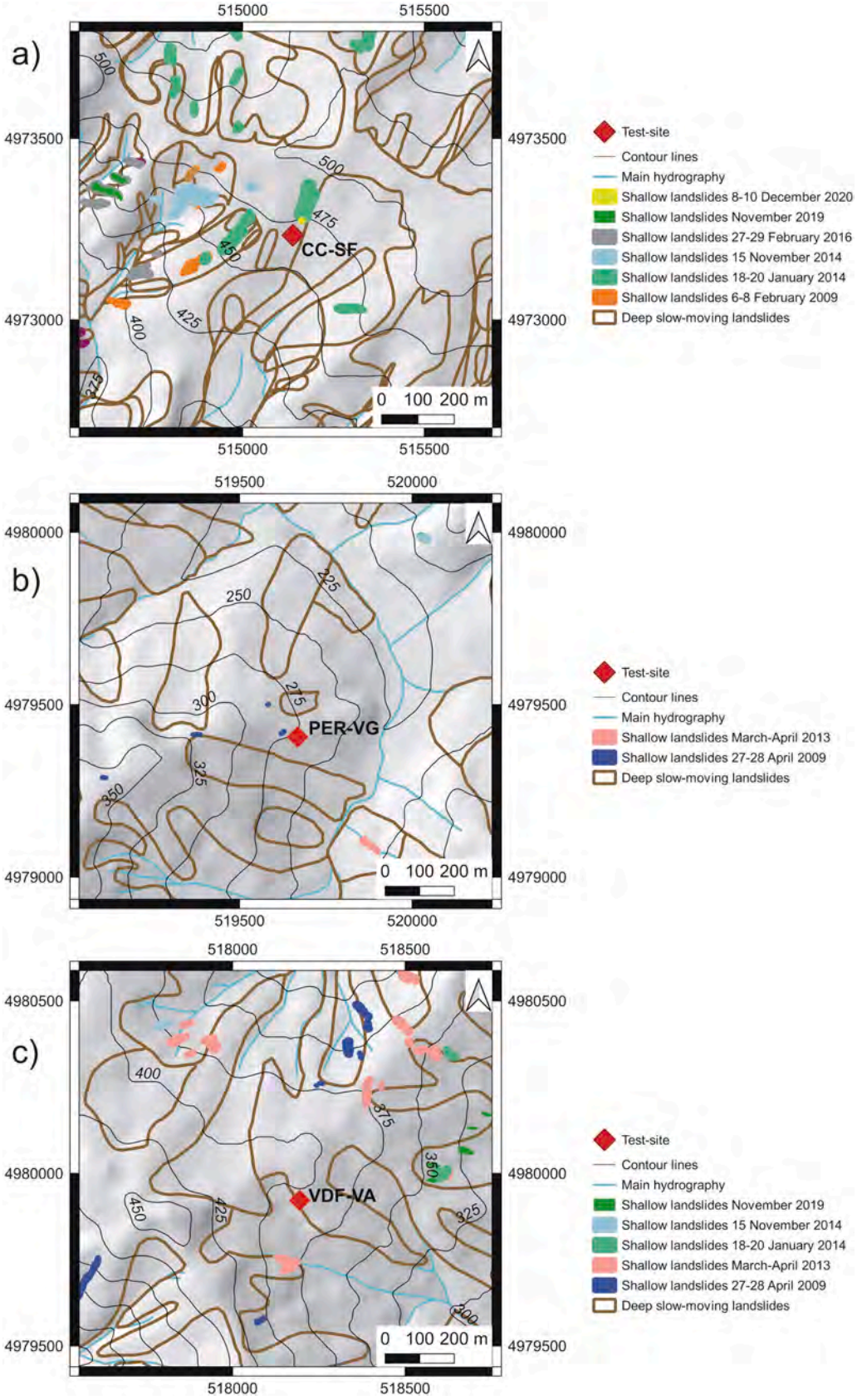

Fig. 2. Detailed geomorphological and landslides distribution settings of the hillslopes where test-sites are located: a) Costa Cavalieri (CC-SF); b) Cascina Pernice (PER-VG); c) Vigna del Fico (VDF-VA).

Table 1
Main geological and geomorphological settings of each test-site.

Test-site	Slope elevation (m a.s.l.)	Slope angle (°)	Slope aspect	Bedrock lithology	Land use	Deep slow-moving landslides	Shallow landslides
CC-SF	450–510	8–18	SW	Clayey melange with block-in-matrix texture	Sowed field (alternance between alfalfa and wheat)	Yes	Yes (6–8 February 2009, 18–20 January 2014, 8–10 December 2020)
PER-VG	250–300	8–15	SE	Marls and arenaceous marls	Vineyard with permanent grass cover in the interrows	No	No
VDF-VA	330–400	7–15	SE	Marls and arenaceous marls	Vineyard with alternation between tillage and grass cover in the interrows	Yes	No

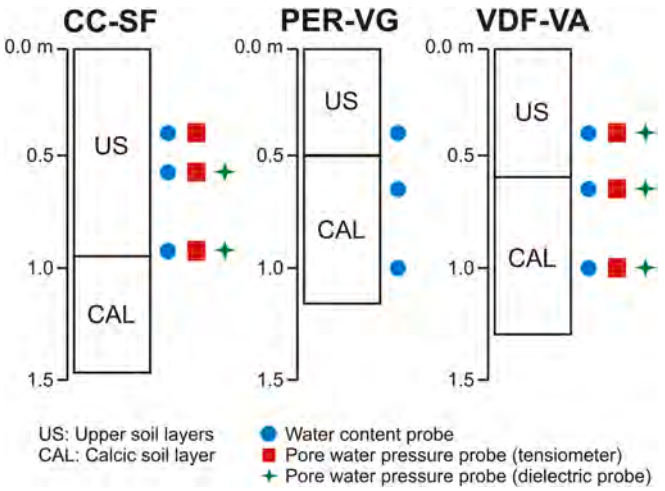

Fig. 3. Soil profiles of the test-sites with indication of the position of water content and pore water pressure probes.

might be present down to depths of 0.3–0.4 m from ground level.

Each root's characteristics were determined through manual digitization within a square frame measuring 0.3 × 0.3 m, following the methodology described by Bischetti et al. (2009). This frame was systematically moved across a 1 m^2 along the entire soil vertical profile along a trench wall (Fig. 4). To digitize the roots' geometry, a Geographical Information System (GIS) software, specifically QGIS, was utilized. The application of GIS facilitated the determination of each root's position in terms of depth and lateral distance from the plant trunk, as well as the calculation of its diameter based on the assumption that a root can be approximated as a cylinder with a circular cross-section (Bischetti et al., 2009).

Root distribution measurements were conducted at 9 different locations in the CC-SF area, while the same parameter was assessed at 6 and 18 points in the PER-VG and VDF-VA areas, respectively. These measurements were taken at varying distances ranging from 0.3 to 1.5 m from the plant trunk. The calculation of root mechanical reinforcement (c_r) was then performed at specific soil depths by integrating the contributions of all the observed roots down to the chosen levels. These levels were selected at distances of 0.5, 1, and 1.5 m from ground level, as they were deemed representative of various factors: 0.5 m represented the highest density of roots in the soil, 1 m corresponded to the typical sliding surface depths of shallow landslides in the study area, and

Table 3
Parameters required for the application of RBMw: F_0 and ξ are the fitting parameters of tensile force at rupture-diameter function; E_0 and β are the fitting parameters of Young's modulus-diameter function; L_0 and α are the fitting parameters of root length-diameter function; λ is the scale Weibull parameter; χ is the shape Weibull parameter.

Parameters of RBMw	CC-SF (sowed fields)	PER-VG and VDF-VA (vineyards)
F_0 (N)	14.02	9.25
ξ (−)	1.92	1.93
E_0 (MPa)	80.20	126.46
β (−)	−0.57	−0.62
L_0 (mm)	101.03	102.04
α (−)	0.79	0.81
r (−)	0.50	0.50
λ (−)	1.02	1.06
χ (−)	1.51	1.64

Fig. 4. Adpoted frame for root-wall technique.

Table 2
Main soil properties of the different layers of each test-site: Gravel) gravel content; Sand) sand content; Silt) silt content; Clay) clay content; LL) liquid limit; PI) plasticity index; γ) unit weight; $CaCO_3$) carbonate content; K_s) saturated hydraulic conductivity; US) upper soil layers; CAL) calcic soil layer.

Test-site	Soil level	Depth (m)	Gravel (%)	Sand (%)	Silt (%)	Clay (%)	LL (%)	PI (%)	γ (kN/m^3)	$CaCO_3$ (%)	K_s (m/s)
CC-SF	US	0.0–0.9	0.5–1.0	2.2–2.3	39.7–45.7	51.5–57.5	69.2–73.9	49.3–53.6	18.6–19.0	9.8–13.7	$1.0{\cdot}10^{-5}$
	CAL	0.9–1.4	2.5	3.2	46.8	47.5	65.5	45.6	20.3	26.7	$1.0{\cdot}10^{-6}$
PER-VG	US	0.0–0.5	12.6–13.5	4.6–4.7	42.6–43.4	39.2	62.4	38.9	19.0–19.3	13.0–15.0	$2.3{\cdot}10^{-6}$
	CAL	0.5–1.2	8.6	2.0	50.3	39.2	58.5	38.3	20.3	21.0	$1.0{\cdot}10^{-6}$
VDF-VA	US	0.0–0.6	0.8–4.5	3.2–4.2	32.0–56.6	39.2–59.4	56.9–69.0	36.8–43.2	18.1–20.1	24.0–28.0	$8.8{\cdot}10^{-5}$
	CAL	0.6–1.3	4.0	4.3	41.6	50.1	47.5	29.1	21.0	36.0	$3.2{\cdot}10^{-5}$

1.5 m denoted the lowest rooting depth in the soil profiles (Bordoni et al., 2019). Furthermore, c_r was quantified at each root density measuring point to assess potential heterogeneities within each test site.

The statistical significance of differences in c_r between different land uses was assessed using a two-way analysis of variance (two-way ANOVA), employing a mixed-effects model. This model considered land use and position along the hillslope as fixed effects, while a root property's values were specified as the random effect. The analysis also included an examination of the significance of the interaction between land use and position along the hillslope within the resulting random effect.

To ensure the validity of the two-way ANOVA, the normality and variance homogeneity of the residualswere assessed using Shapiro-Wilk's and Levene's tests, respectively. The results of these tests, with significance levels (*p*-values) ranging from 0.05 to 0.11, confirmed that the assumptions for applying the two-way ANOVA were met.

All two-way ANOVA analyses were then conducted with a significance level (p-value) of 0.01. In cases where the results of the two-way ANOVA were statistically significant, Tukey's honestly significant difference test was employed to compare the means. This test grouped land uses that did not exhibit statistically significant differences, and again, a significance level (p-value) of 0.01 was utilized for these comparisons.

2.3. Root hydrological reinforcement effect

2.3.1. Field soil hydrological monitoring

Continuous soil hydrological monitoring was conducted across all the test-sites to assess potential variations in hydrological patterns attributable to differing land uses. Detailed information regarding the field equipment used can be found in Table 4.

Meteorological sensors at each test site recorded data on various meteorological parameters, including rainfall, air temperature, air humidity, atmospheric pressure, wind speed and direction, and solar radiation. In the case of PER-VG and VDF-VA, the meteorological station was situated within the vineyards under examination. In contrast, meteorological data for the CC-SF site were obtained from the meteorological station operated by ARPA Lombardia in Fortunago, located 501 m a.s.l. and approximately 2 km away from the test site.

Volumetric soil water content was measured using Frequency-Domain Reflectometer (FDR) probes, which were strategically positioned at three representative soil layers. These layers included the superficial US layer, the middle portion of the soil profile, and the depth typical of shallow landslides' sliding surfaces (Fig. 3). Consequently, FDR probes were installed at depths of 0.4 m, 0.6 m(CC-SF test-site), or 0.7 m (PER-VG and VDF-VA), and 0.9 m (CC-SF test-site) or 1.0 m (PER-VG and VDF-VA) below ground level, respectively.

The analysis and comparison of saturation degree values, derived from the monitored soil water content, provided a more direct means of understanding the differences and similarities in trends observed across different land uses. To achieve this, the trends in soil water content recorded by these probes were transformed into saturation degree trends. This transformation was achieved by calculating the ratio between the measured soil moisture (θ) and the saturated moisture (θ_s). The estimation of saturated moisture was based on laboratory-reconstructed Soil Water Characteristic Curves (SWCCs) for the monitored soil layers (Table 5), employing the Wind Schindler Method technique (Peters and Durner, 2008) using the Hyprop system (UMSGmbH, Munich, Germany). The SWCCs exhibited similar retention properties, as evidenced by the similar values of the α and n fitting parameters of Van Genuchten's (1980) model for the various land uses tested. Additionally, despite sharing similar textural features, θ_s values in the vineyards of the testsites were lower than those observed in the sowed field across different soil horizons.

At corresponding depths, pairs of MPS-6 dielectric sensors and T4e-UMS tensiometers were strategically installed to encompass the entire spectrum of pore water pressure variation (Fig. 3). The MPS-6 sensors were responsible for measuring soil pore water pressure when it fell below −10 kPa, while the T4e-UMS tensiometers handled measurements of pore water pressure exceeding −10 kPa. It is important to note that pore water pressure probes were not deployed in the PER-VG test-site. Additionally, in the CC-SF site, the MPS-6 dielectric sensor was not available at a depth of 0.4 m from the ground.

PER-VG and VDF-VA hydrological sensors acquired data every minute, while CC-SF hydrological probes measured data every 10 min. Average hourly values of measurements were considered to analyse and compare the soil hydrological trends. The analyzed monitoring period of soil water content ranged between 1 August 2020 and 1 September 2022, for a total of 25 months. Since pore water pressure probes were installed at VDF-VA only on 18 May 2021, the analyzed monitoring period of this parameter is referred to the time span between 18 May

Table 4
Hydrological field sensors at the test sites.

Parameter	Device	Model	Depth (m)	Accuracy	Range of measure
CC-SF test-site					
Soil water content	FDR probe	GS3, Decagon Devices Inc., Pullman, WA	0.4, 0.6, 0.9	1 %	0–100 %
Soil pore water pressure (higher than −10 kPa)	Tensiometer	T4e, UMS, Munich, Germany	0.6, 0.9	0.5 kPa	−80/15 kPa
Soil pore water pressure (higher than −10 kPa)	Dielectric sensor	MPS-6, Decagon Devices Inc., Pullman, WA	0.4, 0.6, 0.9	3.0 kPa	−10,000/ −9 kPa
PER-VG test-site					
Soil water content	FDR probe	TerraSense, Netsens, Sesto Fiorentino, Italy	0.4, 0.7, 1.0	2 %	0–100 %
Soil pore water pressure (higher than −10 kPa)	–	–	–	–	–
Soil pore water pressure (higher than −10 kPa)	–	–	–	–	–
VDF-VA test-site					
Soil water content	FDR probe	TerraSense, Netsens, Sesto Fiorentino, Italy	0.4, 0.7, 1.0	2 %	0–100 %
Soil pore water pressure (higher than −10 kPa)	Tensiometer	TEROS 32, Meter, Pullman, WA	0.4, 0.7, 1.0	0.5 kPa	−85/50 kPa
Soil pore water pressure (higher than −10 kPa)	Dielectric sensor	TEROS 21, Meter, Pullman, WA	0.4, 0.7, 1.0	1.0 kPa	−100,000/ −9 kPa

Table 5
Parameters of Van Genuchten (1980)'s model for SWCCs reconstructed at the different monitored depths: θ_s and θ_r are the saturated and residual water contents, respectively; σ and n are the fitting parameters of Van Genuchten (1980)'s model.

Depth of measure (m)	θ_s (m^3/m^3)	θ_r (m^3/m^3)	σ (kPa^{-1})	n (−)
CC-SF test-site				
0.4	0.49	0.01	0.007	1.30
0.6	0.51	0.01	0.017	1.30
0.9	0.51	0.01	0.017	1.30
PER-VG and VDF-VA test-sites				
0.4	0.42	0.03	0.002	1.30
0.7	0.42	0.02	0.006	1.42
1.0	0.41	0.01	0.015	1.27

Table 6
Parameters of Feddes et al.'s (1978) model adopted for the simulation of saturation degree and pore water pressure at the different test-sites.

	Sowed fields (CC-SF)	Alternated vineyards (VDF-VA)	Vineyards with permanent grass cover (PER-VG)
PO (kPa)	0.0	0.0	0.0
POpt (kPa)	0.1	0.1	0.1
P2H (kPa)	−5000.0	−10,000.0	−5000.0
P2L (kPa)	−9000.0	−10,000.0	−10,000.0
P3	−16,000.0	−160,000.0	−160,000.0
r2H (cm/day)	0.5	0.5	0.5
r2L (cm/day)	0.1	0.1	0.1

2021 and 1 September 2022, for a total of about 16 months.

To obtain a reliable comparison between the trends of a hydrological parameter at different land uses, the statistical differences between the trends of the main climatic driving variables (rainfall, air temperature) were evaluated with the Spearman's correlation coefficient (r) and the Nash and Sutcliffe (1970) (NS) statistical indexes and Kruskal-Wallis test for *p*-value of 0.01. The same statistics and test with similar significance level was applied to assess statistical differences or similarities between the trends of a monitored hydrological variable at the different land uses. If the differences were statistically significant, the Dunn test was applied within the groups at p-value of 0.01.

2.3.2. Modelling soil hydrological trends

The HYDRUS-1D code, Version 4.16 (Simunek et al., 2012), was employed to simulate trends in soil pore water pressure at a daily resolution corresponding to various test-sites. The simulations of hydrological trends at a one-dimensional scale were found to be in alignment with the actual field test site configurations. This alignment stemmed from the fact that field measurement devices were strategically positioned along a vertical (one-dimensional) profile. Additionally, the one-dimensional scale was consistent with both the uniform distribution of soil horizons, along with their respective physical and hydrological properties across each hillslope, and the restricted soil thicknesses (ranging from 1.2 to 1.4 m), which primarily facilitated vertical water flow (Bordoni et al., 2021).

The simulated time frame covered the period between 1 June 2021 and 1 September 2022, to enable a comparison between the modelled and field-measured trends of pore water pressure at various depths. These modelled trends were subsequently compared to the actual field trends of the same parameters at CC-SF and VDF-VA. Meteorological variables, including rainfall and air temperature, were utilized as input data for each test-site. Specific SWCCs and values for saturated hydraulic conductivity at each test-site were considered (Tables 2 and 5). Additionally, the impact of plant transpiration was accounted for through Root Water Uptake (RWU), which was influenced by the specific land use present at each test-site. The RWU was modelled following the approach outlined in Feddes et al. (1978), with parameters for each analyzed land use detailed in Table 6. As this model assumed uniform water uptake across depth due to an even distribution of root density, the original input parameters were fine-tuned using data from Taylor and Ashcroft (1972) and Wesseling et al. (1991). This calibration process aimed to derive the most accurate values, considering the nonlinear trends in root density associated with the tested land uses (Bordoni et al., 2020) and to generate modelled trends for soil hydrological parameters that closely resembled the actual monitored data.

The reliability of the modelled trends was evaluated using the r and NS indices. When the modelled trends exhibited a strong correspondence with the actual measurements across various depths, the same modelling approach was applied to recreate pore water pressure trends at depths of 0.4, 0.7, and 1.0 m from the ground level at PER-VG for the same period. Furthermore, pore water pressure trends for the same modelling period were also reconstructed under bare soil conditions, assuming the presence of soil with physical and hydrological characteristics similar to those of the test sites (Tables 2 and 5) and excluding the influence of RWU. Subsequently, all these modelled trends were subjected to statistical comparisons with the measured trends of the same variable. The statistical analysis was performed using Kruskal-Wallis and Dunn tests, with a significance level set at 0.01.

2.3.3. Quantification of the root hydrological reinforcement effect

The root hydrological reinforcement effect (ch_r), induced by RWU of the plants present in a particular land use, is related to the withdrawal of water from the soil to satisfy plant physiological needs and transpiration into the atmosphere (Rodriguez-Iturbe and Porporato, 2004). These induce the reduction of the soil saturation as well as the pore water pressure, potentially increasing the soil shear strength (Gonzalez-Ollauri and Mickovski, 2017; Ng et al., 2020). In these terms, ch_r can be quantified as a pore water pressure difference between a vegetated and a reference bare soil at a certain depth (Person, 1995; Gonzalez-Ollauri and Mickovski, 2017).

For each test-site, daily trends of ch_r were reconstructed for each monitored or modelled soil depths of a particular land use, using an empirical relationship between ch_r and the pore water pressure (ψ_i) (Fredlund et al., 1978; Simon and Collison, 2002) (Eq. (1)):

$$ch_{r,i} = \begin{cases} \psi_i tan\partial\, \psi_i < 0 \\ 0\ \psi_i \geq 0 \end{cases} \quad (1)$$

where δ was the conversion rate between measured pore water pressure and the hydrological reinforcement effect and was set equal to 20° for soil where saturated conditions could occur just in particular seasons of a year (Simon and Collison, 2002), like the ones present in Oltrepò Pavese area (Bordoni et al., 2021). These trends allowed evaluating the plant hydrological reinforcement effect throughout different seasons and different dry and wet periods, highlighting also differences in this contribution between different land uses. ch_r trends were also compared to each other statistically by Kruskal-Wallis and Dunn tests at *p*-value of 0.01, as for the other comparisons between hydrological trends.

2.4. Effect of root reinforcement on shallow slope stability

Slope stability analyses towards rainfall-induced shallow landslides were carried out to assess the effect of different types of root reinforcements on the proneness of failure for a particular vegetated slope, according to the analyzed land uses.

A simplified slope stability model based on the infinite slope theory (Baum et al., 2008) was used to calculate the slope safety factor (Fs) trends at the typical depth of development of shallow sliding surfaces (1

m) during the period between 1 June 2021 and 1 September 2022, through Eq. (2):

$$Fs = \frac{tan\varphi'}{tan\omega} + \frac{C - \psi\gamma_w tan\varphi'}{\gamma z sin\omega cos\omega} \quad (2)$$

where φ' is the soil friction angle, C is the soil cohesion, ψ is the soil pore water pressure, γ_w is the unit weight of the water, ω is the slope angle, γ is the unit weight of the soil and z is the depth below the ground level at which a potential sliding surface could develop. In this formulation, the term C is the result of the sum between the soil effective cohesion c' and a root reinforcement term, which could be alternatively a mechanical reinforcement (c_r; Eq. (3)), or a hydrological reinforcement effect (ch_r; Eq. (4))

$$C = c' + c_r \quad (3)$$

$$C = c' + ch_r \quad (4)$$

In the case of Fs of a bare soil, ch_r was equal to 0 kPa, reducing C equal to c'.

The method to evaluate the role that a particular analyzed vegetation plays in improving the slope stability through c_r or ch_r consisted in calculating the percentage of Fs increment (Fs_{In}) compared to the bare soil condition for each scenario (Capobianco et al., 2021) (Eq. (5)):

$$Fs_{In} = 100 \cdot \frac{Fs_V - Fs_B}{Fs_B} \quad (5)$$

where Fs_B is Fs calculated for the condition of bare soil and Fs_V is Fs calculated for each analyzed land use setting. Fs_{In} was calculated for each land use considering only the mechanical contribution of the roots (c_r) or only their hydrological contribution (ch_r), or considering both the effects at the same time.

The slope stability calculations were implemented considering representative values of steepness and typical soil geotechnical parameters of the hillslopes where the analyzed agro-ecosystems are present in the study area. In these scenarios, only c_r or ch_r changed, allowing a more clear representation of the effects induced by the presence of vegetation on slope stability.

3. Results

3.1. Root mechanical reinforcement

Fig. 5 illustrates the trends of calculated c_r values for the soil layers under consideration. The statistical analysis revealed that there were no significant differences in c_r values among the various sampling locations within the same land use category while treating the type of land use as a fixed factor (Table 7). Instead, c_r exhibited statistically significant differences among test sites with varying land use types, as indicated by the data presented in Fig. 5 and Table 7. These differences were further confirmed by the results of a two-way ANOVA analysis ($F_{2,21} = 13.36$, *p*-value <0.01 for c_r at a depth of 0.5 m; $F_{2,21} = 13.56$, p-value <0.01 for c_r at a depth of 1.0 m; $F_{2,21} = 16.16$, p-value <0.01 for c_r at a depth of 1.5 m). Furthermore, Tukey's test results (Table 8) indicated that all pairs of land use categories exhibited statistically significant differences for each soil layer.

VDF-VA exhibited the highest mechanical root reinforcement across all three analyzed soil depths (4.4 ± 1.0 kPa at 0.5 m from the ground, 3.1 ± 0.6 kPa at 1.0 m from the ground, 1.6 ± 0.3 kPa at 1.5 m from the ground). In contrast, PER-VG generally showed c_r values 17–31 % lower than those of VDF-VA, while CC-SF displayed a significant decrease in $c_r$values, averaging 65–71 % lower. Furthermore, c_r values exhibited a downward trend with increasing depth for each analyzed land use, experiencing a reduction of 30–45 % from 0.5 m to 1 m in depth and a decrease of 41–49 % from 1 m to 1.5 m in depth.

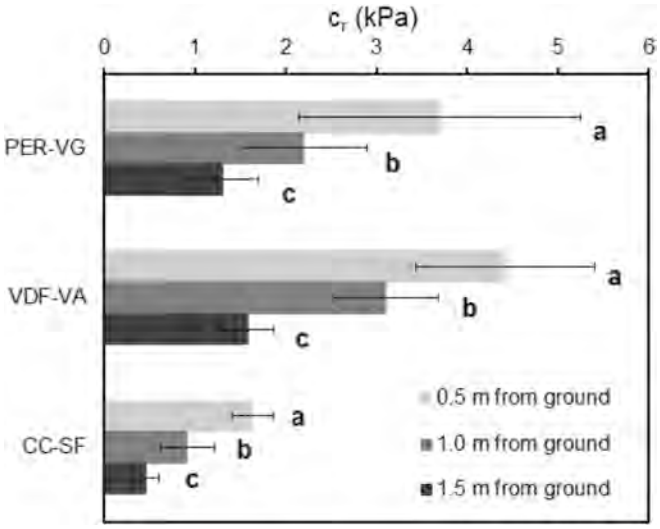

Fig. 5. Mean and standard errors of root mechanical reinforcement (c_r) in the different land uses. Bold letters next to each bar of the different land uses indicate that they were statistically similar by Tukey's test (*p*-value equal to 0.01) considering that particular soil level.

Table 7
Results of Two-way ANOVA tests for mechanical root reinforcement (c_r) tested at different soil depths, considering land use and sample location as fixed effects and, also, the mixed effects of both these features. Significant differences were considered at p-value equal to 0.01 and are identified by bold characters.

Variable	Land use (PER-VG, VDF-VA, CC-SF)		Sample location		Land use × sample location	
	F	p-Value	F	p-Value	F	p-Value
c_r at 0.5 m from ground	13.36	<0.001	0.61	0.44	0.26	0.77
c_r at 1.0 m from ground	13.56	<0.001	0.42	0.52	0.44	0.65
c_r at 1.5 m from ground	16.16	<0.001	0.47	0.50	0.24	0.79

3.2. Monitored soil hydrological trends

To assess the confidence level of field soil hydrological measurements, laboratory tests were conducted to determine the saturation degree of samples collected at varying depths and during different seasons throughout the monitoring period at all test-sites (Fig. 6). The field saturation degree exhibited a high degree of confidence, as evidenced by differences between field measurements and their corresponding laboratory counterparts, which were consistently below 6 % across all test-sites. Additionally, the correlation coefficient (r) and Mean Absolute Error values ranged from 0.91 to 0.94 and 2.78 % to 2.91 %, respectively. Regarding field measurements of soil pore water pressure, Bordoni et al. (2021) demonstrated a high level of confidence in the measurements conducted using the sensors employed at the chosen test-sites. For tensiometers and conditions close to saturation, the differences were <1–2 kPa, while for the dielectric sensors and conditions far from saturation, differences remained below 10–20 kPa. Consequently, the field data can be considered reliable for identifying the key hydrological characteristics of the analyzed sites.

Rainfall amounts and air temperature trends exhibited similarities across the various test-sites (Table 9). This similarity is supported by correlation coefficients (r) and Nash-Sutcliffe efficiency (NS) values exceeding 0.8, following the criteria established by Krause et al. (2005), as well as the results of the Kruskal-Wallis test ($\chi^2 = 4.15$, *p*-value = 0.21 for air temperature; $\chi^2 = 3.25$, p-value = 0.20 for rainfall). Notably, the monitoring period was marked by two anomalous periods. The period

Table 8
Comparisons between the pairs of the land uses through the application of Tukey's test for mechanical root reinforcement (c_r). Pairs that are statistically similar according to Tukey's test results (p-value equal to 0.01) are in bold characters.

Pair	0.5 m from ground		1.0 m from ground		1.5 m from ground	
	Difference between the means (mean ± standard error) kPa	p-Value	Difference between the means (mean ± standard error) kPa	p-Value	Difference between the means (mean ± standard error) kPa	p-Value
PER-VG/ VDF-VA	−0.7 ± 0.6	<0.001	−0.9 ± 0.1	<0.001	−0.3 ± 0.1	<0.001
PER-VG/ CC-SF	2.1 ± 1.3	<0.001	1.3 ± 0.4	<0.001	0.8 ± 0.3	<0.001
VDF-VA/ CC-SF	2.8 ± 1.3	<0.001	2.2 ± 0.3	<0.001	1.1 ± 0.2	<0.001

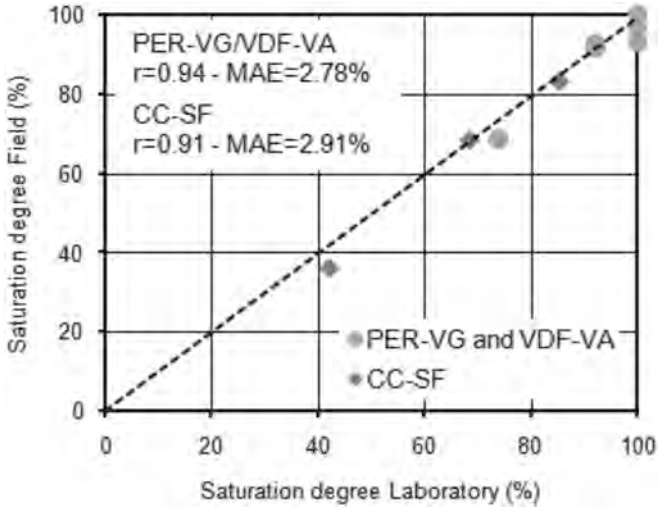

Fig. 6. Comparison between laboratory and corresponding field measurements of saturation degree at different test-sites.

between December 2020 and January 2021 was exceptionally rainy, with a cumulative rainfall ranging from 363 to 428.4 mm. This amount was 412 % to 487 % higher than the average of 87.9 mm recorded for the same period from 1999 to 2021, as reported by the Fortunago station within the ARPA Lombardia monitoring network. In contrast, the period spanning from December 2021 to August 2022 experienced notably hotter and drier conditions than the average conditions until June 2022. From December 2021 to February 2022, the average temperature ranged from 5.2 to 5.5 °C, accompanied by cumulative rainfall amounts of 54.6 to 70.4 mm. Subsequently, from March 2022 to June 2022, the average temperature was 15.2 to 15.8 °C, with cumulative rainfall measuring between 95.8 and 107.7 mm. These periods were 1.5 °C to 1.8 °C warmer and saw rainfall levels reduced by 46 % to 60 % compared to the average conditions observed from 1999 to 2021 at the Fortunago station. Additionally, the period of July to August 2022 also stood out as significantly warmer than the average conditions, with temperatures ranging from 25.2 °C to 25.8 °C, representing an increase of 2.4 °C to 3.0 °C.

Figs. 7 and 8 depict the trends in saturation degree and pore water pressure at various test sites, corresponding to different depths. These parameters exhibited distinct dynamics across different layers and land uses, as evidenced by the low values of the correlation coefficients (r, lower than 0.7) and Nash-Sutcliffe (NS) indexes (lower than 0.1), following the criteria outlined by Krause et al. (2005). The statistical significance of these differences was confirmed by the results of the Kruskal-Wallis test (χ^2 = 12,228–16,493, p-value<0.001 for saturation degree; χ^2 = 70.18–729.65, p-value<0.001 for pore water pressure; Fig. 6–7) and the Dunn test (Z scores for all pairs ranging from 11.47 to 80.47, p-value<0.001). It is worth noting that all sensors required approximately one month to re-equilibrate with the soil, as reported by Bordoni et al. (2021). Therefore, the initial months of the monitoring period (August 2020 for saturation degree and May 2021 for pore water pressure) were not considered representative of the actual soil conditions during those time spans.

In the uppermost soil layers (0.4 m from ground level), the saturation

Table 9
Values of the indexes (Spearman's correlation coefficient r and Nash and Sutcliffe index NS) used for estimating the similarity between the trends of different meteorological and soil hydrological parameters.

	PER-VG	VDF-VA	CC-SF
Air temperature			
r (−)			
PER-VG		0.88	0.83
VDF-VA			0.86
NS (−)			
PER-VG		0.88	0.81
VDF-VA			0.83
Cumulated rainfall			
r (−)			
PER-VG		0.90	0.81
VDF-VA			0.84
NS (−)			
PER-VG		0.87	0.80
VDF-VA			0.82
Water content-0.4 m			
r (−)			
PER-VG		0.62	0.55
VDF-VA			0.39
NS (−)			
PER-VG		0.08	0.13
VDF-VA			0.10
Water content-0.7 m			
r (−)			
PER-VG		0.67	0.60
VDF-VA			0.60
NS (−)			
PER-VG		0.07	0.03
VDF-VA			0.05
Water content-1.0 m			
r (−)			
PER-VG		0.29	0.66
VDF-VA			0.33
NS (−)			
PER-VG		0.01	0.04
VDF-VA			0.03
Pore water pressure − 0.7 m			
r (−)			
PER-VG		–	–
VDF-VA			0.30
NS (−)			
PER-VG		–	–
VDF-VA			0.04
Pore water pressure − 1.0 m			
r (−)			
PER-VG		–	–
VDF-VA			0.24
NS (−)			
PER-VG		–	–
VDF-VA			0.03

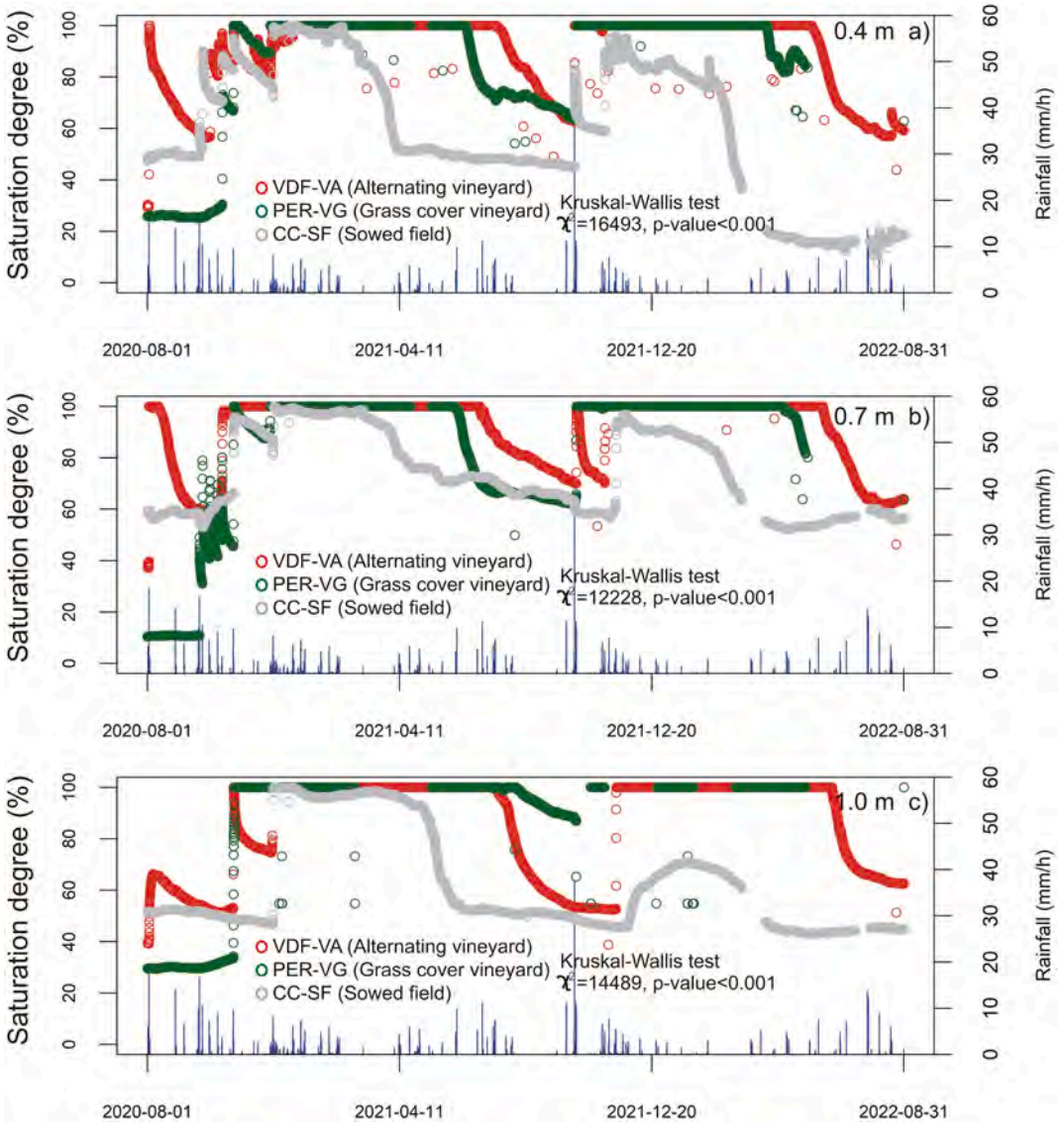

Fig. 7. Trends of saturation degree monitored in different test-sites at 0.4 (a), 0.7 (b) and 1.0 m (c) from ground.

degree and pore water pressure dynamics exhibited a close relationship with short-term rainy and dry periods. These changes in hydrological parameters occurred much more rapidly than those observed in the deeper monitoring levels. During hot and dry periods, which typically span from May to September, the saturation degree at 0.4 m was, on average, 24–33 % higher in vineyards than in cultivated fields. This difference was less pronounced for pore water pressure, with both CC-SF and VDF-VA sites showing similar values, reaching approximately −1500 kPa during the May–September period. Rainfall events during the first week of October 2021 led to a rapid increase in soil water content across all monitored test-sites. This increase was evident through the rise in saturation degree, reaching close to 100 %, and a decrease in pore water pressure to below −10 kPa. However, in the subsequent days of October, when there was no rainfall, soil water content in sowed fields further decreased. The saturation degree dropped to around 60 %, and pore water pressure decreased to as low as −110 kPa. In contrast, the vineyard test-sites did not experience the same phenomenon. They maintained conditions close to complete saturation, with saturation degree and pore water pressure remaining near 100 % and 0 kPa, respectively.

These distinct behaviours were also observed throughout the remainder of the autumn (November) and the winter months (December–February). Although pore water pressure under −9 kPa could not be measured at CC-SF due to the absence of a tensiometer, the monitored sowed fields exhibited more pronounced fluctuations in saturation degree and pore water pressure during this period. This was evident in the alternation between conditions close to complete saturation and extended periods of unsaturated conditions during intervals without significant rainfall. Specifically, the saturation degree ranged between 72 % and 85 %, and pore water pressure fluctuated between −60 and −20 kPa. In contrast, the soil in both of the tested vineyards maintained consistently saturated conditions during these same periods, with pore water pressure staying within the narrow range of −5 to 0 kPa. This pressure occasionally increased into the positive range (up to 0.9 kPa) during the most significant rainfall events, which typically exceeded 20 mm/day. On average, the saturation degree at a depth of 0.4 m in the November–February period was 7–11 % higher in the vineyards compared to the sowed fields.

During the spring months of March and April, distinct hydrological dynamics were observed at a depth of 0.4 m in the three tested land uses. Sowed fields (CC-SF) exhibited a similar hydrological pattern to that observed from November to February until the early part of March. It was during this period that both soil saturation degree and pore water pressure began a continuous decline, ultimately reaching their lowest

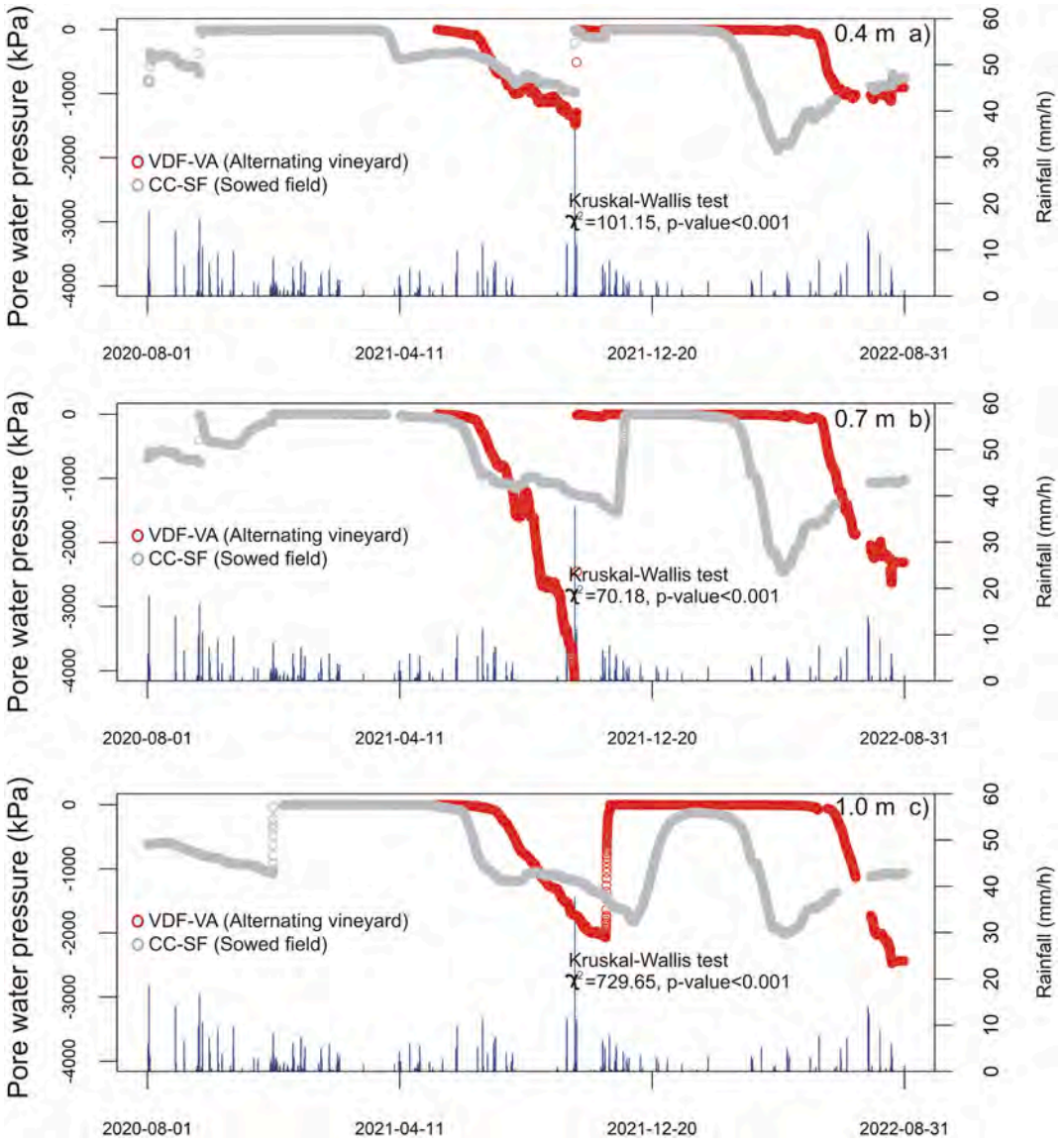

Fig. 8. Trends of pore water pressure monitored in different test-sites at 0.4 (a), 0.7 (b) and 1.0 m (c) from ground.

values during the summer months. This transition point corresponded to 7 March 2021 and 2 March 2022 in the two monitored years.

Conversely, the hydrological patterns observed from November to February remained relatively stable for a more extended duration in the monitored vineyards. This constancy persisted until the latter half of April for the vineyard with permanent grass cover (starting points in 26 April 2021–17 April 2022 at PER-VG) and until the first half of May for the vineyard with alternating interrow management of the inter-row (starting points in 16 May 2021–19 May 2022 at VDF-VA). Furthermore, it is worth noting that the driest soil conditions were reached earlier in the vineyard with permanent grass cover (by the end of May) than in the vineyards with alternating management (beginning of July). Based on these observed behaviours, vineyards with alternating management maintained a saturation degree that was, on average, 12 % and 28 % higher compared to vineyards with permanent grass cover and sowed fields, respectively.

The hydrological dynamics at soil depths of 0.7 and 1 m exhibited distinct patterns. The re-wetting of these soil horizons commenced in autumn (October–November) and was as rapid as observed in the shallower layers, albeit occurring earlier in vineyards compared to sowed fields. Notably, the re-wetting process until conditions approximating saturation at a depth of 0.7 m occurred at PER-VG and VDF-VA following intense rainfall events, typically characterized by at least 70 mm of rain within50 hours. In these locations, a similar re-wetting at a 1-m depth from the ground surface occurred after two weeks of cumulative rainfall exceeding 100 mm. Following re-wetting, these layers approached conditions very close to saturation, with a saturation degree exceeding 97 % and pore water pressure ranging between −10 and 0 kPa. At VDF-VA, positive pressures developed at both 0.7 and 1-m depths in response to rainfall events with at least 30 mm/day of cumulative rainfall.

In the monitored sowed field (CC-SF), a comparable re-wetting process occurred at depths of 0.6–0.7 m and 0.9–1 m from the ground surface, happening nearly simultaneously during rainy periods with 100 mm of cumulative rainfall over 10–15 days. Subsequently, these layers reached conditions close to complete saturation, with a saturation degree exceeding 95 % and pore water pressure higher than −5 kPa, throughout the remainder of autumn and winter. Positive pressures increased, reaching up to 5 kPa at 0.7 m and 8.6 kPa at 0.9 m, coinciding with rainfall events of at least 20 mm/day. Due to these divergent behaviours, vineyards with permanent grass cover exhibited saturation degrees at depths of 0.7 and 1 m from the ground surface during the

November–February period that were, on average, higher by 3–4 % and 26–32 % compared to vineyards with alternating management cover and sowed fields, respectively.

The behaviour during the coldest and rainiest months persisted for varying durations across different land uses. In sowed fields, the decline in saturation degree and pore water pressure commenced in the middle of March to the early days of April (starting points in 1 April-6 April 2021, 15–21 March 2022). In contrast, in vineyards, this decline started later, occurring between the latter half of May and the beginning of June for the vineyard with permanent grass cover (10 June 2021–20 May 2022) and between the latter half of June and the latter half of July for the vineyard with alternating management (1–18 July 2021, 11–21 June 2022). As a result of these disparities in behaviour, vineyards with alternating management maintained saturation degrees at 0.7 and 1 m from the ground during the March–October period that were, on average, 5–12 % and 33–40 % higher than those in vineyards with permanent grass cover and sowed fields, respectively.

3.3. Modelled soil pore water pressure trends

The trends of the pore water pressure modelled with HYDRUS-1D at CC-SF and VDF-VA (Fig. 9) exhibited strong agreement with the observed trends across all analyzed soil depths. The values of the r and NS indexes were relatively high, ranging from 0.81 to 0.91 for r and 0.79 to 0.88 for NS, which confirms the effectiveness of the modelling scheme (Krause et al., 2005). The modelled trends accurately simulated the hydrological dynamics observed at various depths during both dry and rainy periods in CC-SF and VDF-VA.

However, it is worth noting that the model's trend at a depth of 0.9 m in CC-SF indicated conditions close to complete saturation (lower than −10 kPa) during the period from December 2021 to March 2022. These conditions were not reflected in the actual measurements, which consistently remained below −100 kPa throughout this period. Furthermore, during August–September 2021, extreme negative values of pore water pressure were recorded in all monitored layers at VDF-VA. These values were significantly higher (ranging from 230 to 680 kPa) than the measurements obtained by the model for the same months.

Given the reliability of the modelled pore water pressures at the CC-SF and VDF-VA test sites, it was decided to also utilize the modelled trends of pore water pressure at depths of 0.4, 0.7, and 1 m from the ground level for both bare soil conditions and PER-VG (Fig. 10) during the same period. Similar to the trends observed in other land uses, the dynamics of pore water pressure in bare soil indicated a significant decrease in soil saturation and corresponding pore water pressure during the hot and dry season, especially between April and September. Conversely, there was a re-wetting trend, leading to conditions close to complete saturation during the wet season, primarily occurring between November and March.

Despite exhibiting similar dynamics, the pore water pressure in the bare soil did not reach the lowest values observed in the cultivated fields and vineyards. In fact, during July–August 2022, the pore water pressure in the bare soil did not drop below −1040/−770 kPa. In contrast, values below −2000 kPa were recorded in the other land uses. Regarding the vineyard with permanent grass cover represented by PER-VG, the pore water pressure dynamics at various depths exhibited trends similar to those observed at the same depths in VDF-VA (vineyard with

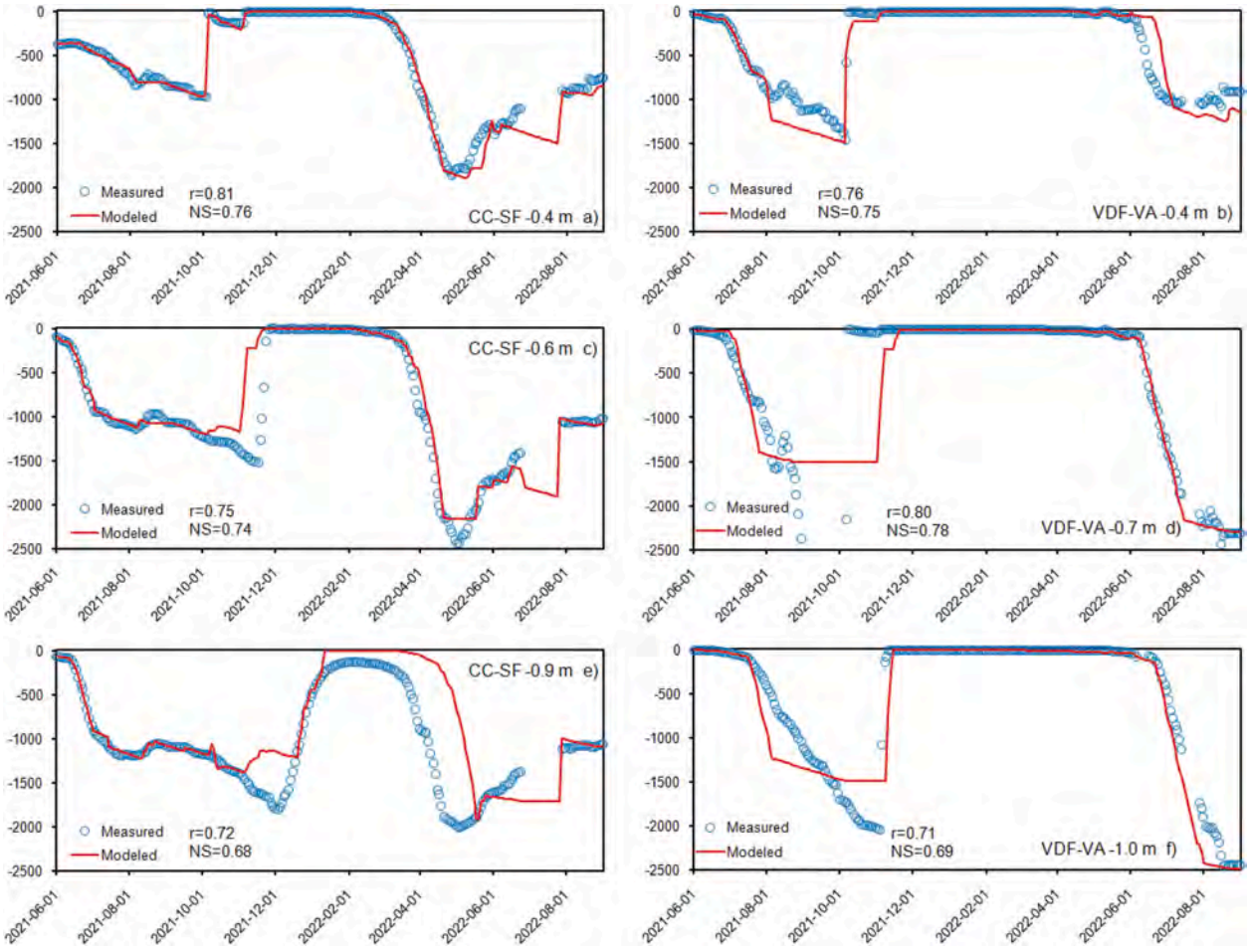

Fig. 9. Comparison between modelled and monitored trends at 0.4 m from ground in CC-SF (a) and VDF-VA (b), 0.7 m from ground in CC-SF (c) and VDF-VA (d), 1.0 m from ground in CC-SF (e) and VDF-VA (f).

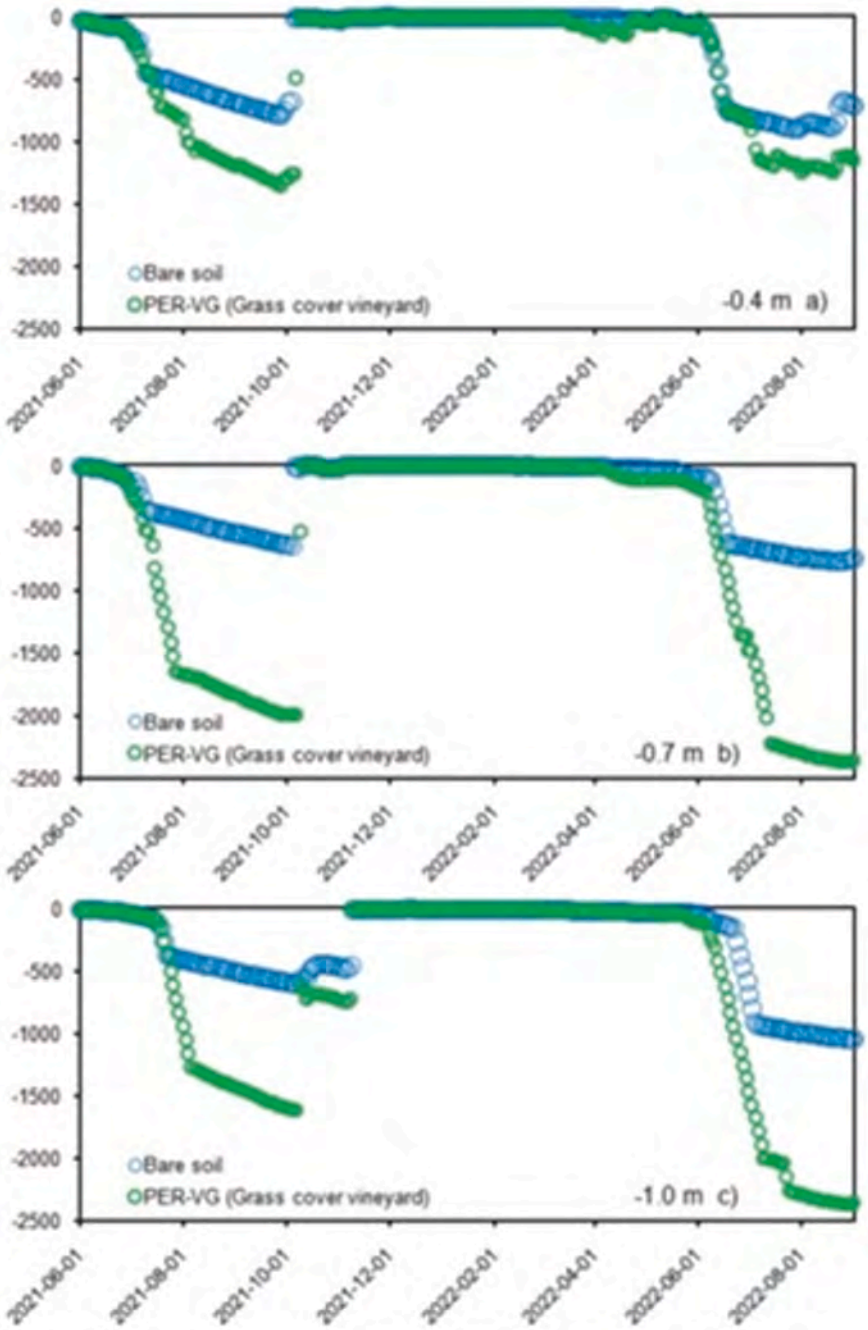

Fig. 10. Modelled trends of pore water pressure for a bare soil and PER-VG site at 0.4 (a), 0.7 (b) and 1.0 (c) m from the ground level.

alternating management). Similar values of pore water pressure, close to 0 kPa, were observed during the November–March period, while the lowest values were simulated during the hot season, particularly in August and September.

The differences in pore water pressure trends observed among the analyzed land uses were further confirmed through statistical analysis using the Kruskal-Wallis test ($\chi^2 = 62.53$ for 0.4 m, $\chi^2 = 92.05$ for 0.7 m, and p-value $= 187.99$ for 1.0 m, with a p-value <0.001). Subsequent Dunn tests also indicated significant distinctions between all pairs, with Z-values ranging from -13.04 to 10.08 and p-values falling between <0.001 and 0.002.

3.4. Root hydrological reinforcement effect

The daily trends of ch_r at the three test sites, each with different land uses, were reconstructed using Eq. (1) for the period between 1 June 2021 and 31 August 2022, corresponding to the three monitored depths along the soil profile (Fig. 11). The trends of ch_r exhibited statistically significant differences among the various land uses within each analyzed soil layer (Kruskal-Wallis test results: $\chi^2 = 60.74$ for 0.4 m, $\chi^2 = 27.33$ for 0.7 m, p-value $= 56.29$ for 1.0 m, p-value <0.001; Dunn test results: Z scores for all pairs ranged between 1.25 and 7.80, with p-values <0.01).

The ch_r values for all the considered land uses reached their highest levels between June and October. While rainfall-induced shallow landslides rarely occurred during this period due to dry soil conditions, ch_r values exceeded 10^2 kPa during these months. The most significant variations in ch_r were observed in the shallowest layer (0.4 m from the ground), where shallow landslide surfaces typically do not develop. These variations were associated with periodic decreases immediately

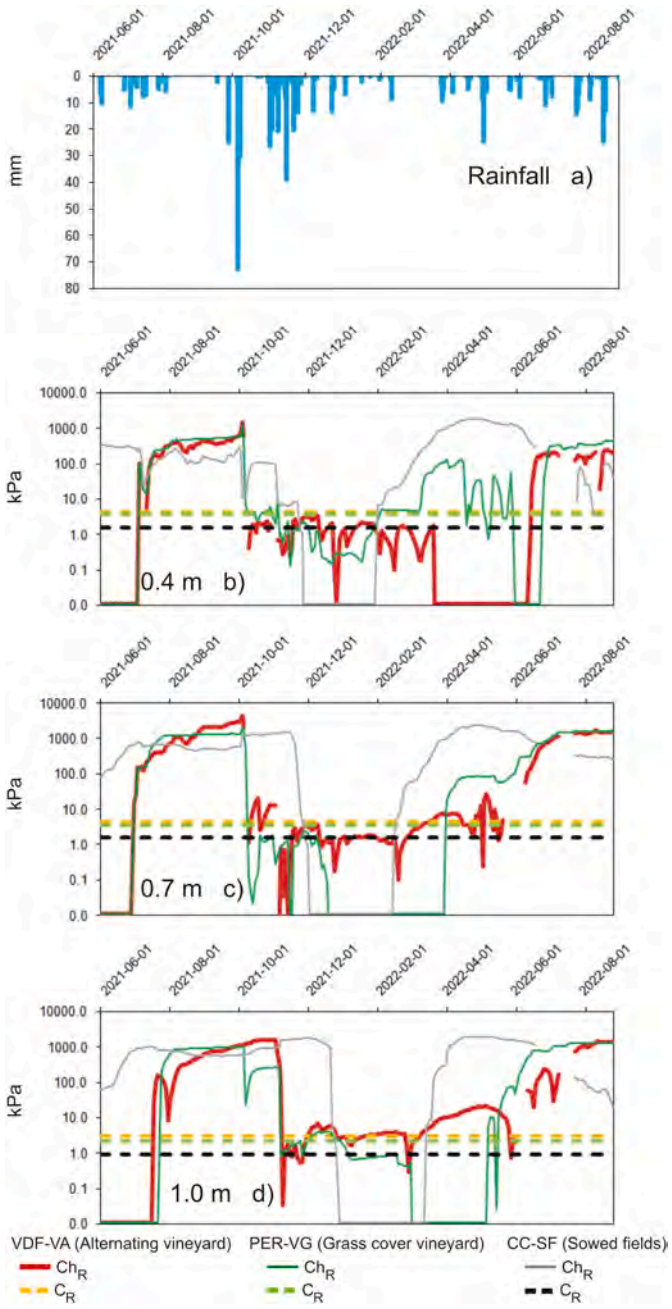

Fig. 11. Calculated daily root hydrological reinforcement (ch_r) trends at different depths in soil profiles: a) rainfall amounts; b) ch_r at 0.4 m from ground; c) ch_r at 0.7 m from ground; d) ch_r at 1.0 m from ground.

following intense thunderstorms, which led to rainwater infiltration at this level (at least 20 mm/day). The highest ch_r values were recorded in vineyards at depths of 0.7 and 1.0 m, where values higher than 10^3 kPa (reaching up to 1323.7–1982.6 at PER-VG and 1561.6–2897.6 kPa at VDF-VA) were observed in August and September. In sowed fields, the highest ch_r values occurred in June at depths of 0.7–1.0 m but did not exceed 1977.7 kPa. The increase in ch_r during the hot season was rapid across all the analyzed land uses, with changes ranging from values close to 1 kPa to over 10^3 kPa occurring within 15–23 days. However, these changes occurred at different times, starting in April–May in sowed fields, the second half of May in vineyards with permanent grass cover, and the first half of June in vineyards with alternating management.

The decline in ch_r began in October–November, coinciding with rainy periods, and initially affected the shallowest layer before impacting deeper layers. Following a cumulative rainfall of 108.3 mm over 4 days between 3 and 6 October 2021, ch_r values for all land uses decreased to levels between 1 and 6 kPa at a depth of 0.4 m. During the most substantial rainy periods in autumn and winter (at least 20 mm of rain in one day), ch_r dropped further below 1 kPa. In December and January, ch_r levels in sowed fields remained negligible for all monitored soil depths, while in vineyards, they ranged between 1.5 and 0.2 kPa during the same period, reaching negligible conditions only at the end of January and the first half of February. In the deeper layers (0.7 and 1.0 m from the ground), ch_r fell below 1 kPa only in the first half of November, following cumulative rainfall of at least 130 mm over 15 days. After this event, ch_r dynamics in different land uses mirrored those observed at a depth of 0.4 m, with values reaching 0 kPa in sowed fields in December and in the first half of January in vineyards.

The ch_r values for sowed fields began to rise throughout the entire soil profile in early March, transitioning from values of 10^1 kPa to levels exceeding 10^3 kPa within 28–30 days. These elevated values persisted for the remainder of the spring months, except for occasional drops below 10 kPa during intense rainfall events (e.g., 33.5 mm of rain between 5 and 6 May 2022). In contrast, ch_r remained below 10 kPa until the first half of May in vineyards with permanent grass cover and until the beginning of June (a difference of 16–18 days) in vineyards with alternating management. Nil values were recorded during intense rainfall events (e.g., 39.4 mm of rain between 5 and 8 May 2022). After these time intervals, ch_r increased to levels exceeding 10^3 kPa within 22–25 days.

Assuming that root mechanical reinforcement remained consistent throughout different seasons in this context, as demonstrated in Bordoni et al. (2016) for grapevine plants, the average $c_r$values for each land use at different depths are presented in Fig. 11. This allows for a comparison between the mechanical and hydrological reinforcement effects. Across all analyzed land uses, hydrological reinforcement was, on average, 10–100 times higher than mechanical reinforcement during the period from June to September. It is worth noting that the likelihood of shallow landslides during these months is very low due to the dry soil conditions.

As the soil re-wetted between October and November, ch_r initially exhibited similar or only 2–3 times higher values than the corresponding c_r values in all tested land uses. However, ch_r values became lower than c_r when the soil approached or reached complete saturation during the rainiest periods between November and February. During the period from March to May, ch_r surpassed c_r at the beginning of March in sowed fields and in the first half of May to the beginning of June in vineyards. Nevertheless, ch_r in all tested land uses could drop below the average c_r during intense rainfall events occurring in these months (e.g., 39.4 mm of rain between 5 and 8 May 2022).

3.5. Slope safety factor trends

The effects of root reinforcement on the safety factor of slopes (Fs) were investigated by reconstructing daily trends during the same period in which pore water pressure was modelled and quantifying root hydrological reinforcement. Fs was calculated using Eq. (2) for the analyzed land uses, taking into account the trends in pore water pressure. As previously explained, pore water pressure was measured for sowed fields and alternating vineyards, while it was modelled with HYDRUS-1D for bare soils and vineyards with grass cover. Fs scenarios were estimated, considering root mechanical reinforcement, root hydrological reinforcement, or the absence of both. The latter condition represents bare soil. To facilitate a better comparison of the impacts of these reinforcements on different land uses, we considered the same set of geological and geomorphological parameters required for solving Fs, as listed in Table 10.

Daily trends of Fs (Fig. 12) highlighted the significant role of root reinforcement in enhancing shallow slope stability. In unsaturated soil conditions with pore water pressure below −10 kPa, Fs consistently exceeded 1 (indicating stability) and even exceeded 100 during dry

Table 10
Parameters used on slope safety factor calculations: φ' and c' are the soil friction angle and the soil effective cohesion, respectively, estimated through direct shear tests; c_r is the mechanical root reinforcement for sowed fields, alternating vineyards and grass covered vineyards; γ_w is the unit weight of the water; γ is the unit weight of the soil; z is the depth below the ground level at which a potential sliding surface could develop;ω is the slope angle.

Parameter	Value
φ' (°)	36
c' (kPa)	2.5
c_r (kPa)-Sowed fields	0.9
c_r (kPa)-Alternating vineyards	3.1
c_r (kPa)-Grass covered vineyards	2.2
γ_w (kN/m^3)	9.8
γ (kN/m^3)	20.3
z (m)	1.0
ω (°)	18

periods until early October (Fig. 12 c, e). These conditions were observed in all analyzed land uses, whether considering c_r or ch_r. When ch_r was incorporated into the model, Fs_{In} exhibited greater significance compared to the bare soil condition (ranging from 5.4 % to 179.3 % considering ch_r; 2.2 % to 9.6 % considering c_r). Among the analyzed agroecosystems, vineyards showed a more substantial increase in FsIn compared to sowed fields (on average, 2.2 % in sowed fields and 5.5 % to 6.8 % in vineyards for c_r; on average, 63.7 % in sowed fields and 78.2 % to 98.3 % in vineyards for ch_r).

The significance of root reinforcement in enhancing slope stability became more pronounced when the soil approached or reached complete saturation (pore water pressure higher than −10 kPa) during rainy periods between November and March. In comparison to the corresponding value for bare soil, Fs_{In} was higher for vineyards than for sowed fields when considering c_r in the Fs calculation (averaging 2.8 %, 7.3 %, and 5.6 % in sowed fields, vineyards with alternating management, and vineyards with grass cover, respectively).

However, when considering ch_r, the increase in Fs values compared to bare soil was significantly more pronounced in vineyards than in sowed fields. On average, daily Fs was only 5.0 % higher in sowed fields than in bare soil conditions, while it increased approximately 3.5 times (350 %) in vineyards with alternating management and around two times (226 %) in vineyards with permanent grass cover compared to bare soil conditions. These differences were particularly notable on days when rainfall events had the potential to elevate pore water pressure to positive values (up to 1.4 kPa), resulting in a decrease in slope Fs (Fig. 12d, f).

Between March and June, Fs calculated with the inclusion of c_r exhibited similar trends, showing an increase compared to bare soil due to the amount of root reinforcement provided by each land use (averaging 2.7 % in sowed fields, 7.2 % in vineyards with alternating management, and 5.1 % in vineyards with grass cover). Conversely, when considering Fs calculated with the inclusion of ch_r, sowed fields displayed higher Fs_{In} values (ranging from 0.0 % to 423.8 %) than vineyards (ranging from 0.0 % to 95.8 %), particularly noticeable between March and the first half of May, when ch_r values in sowed fields reached up to 10^2 kPa while ch_r values in vineyards remained below 10 kPa.

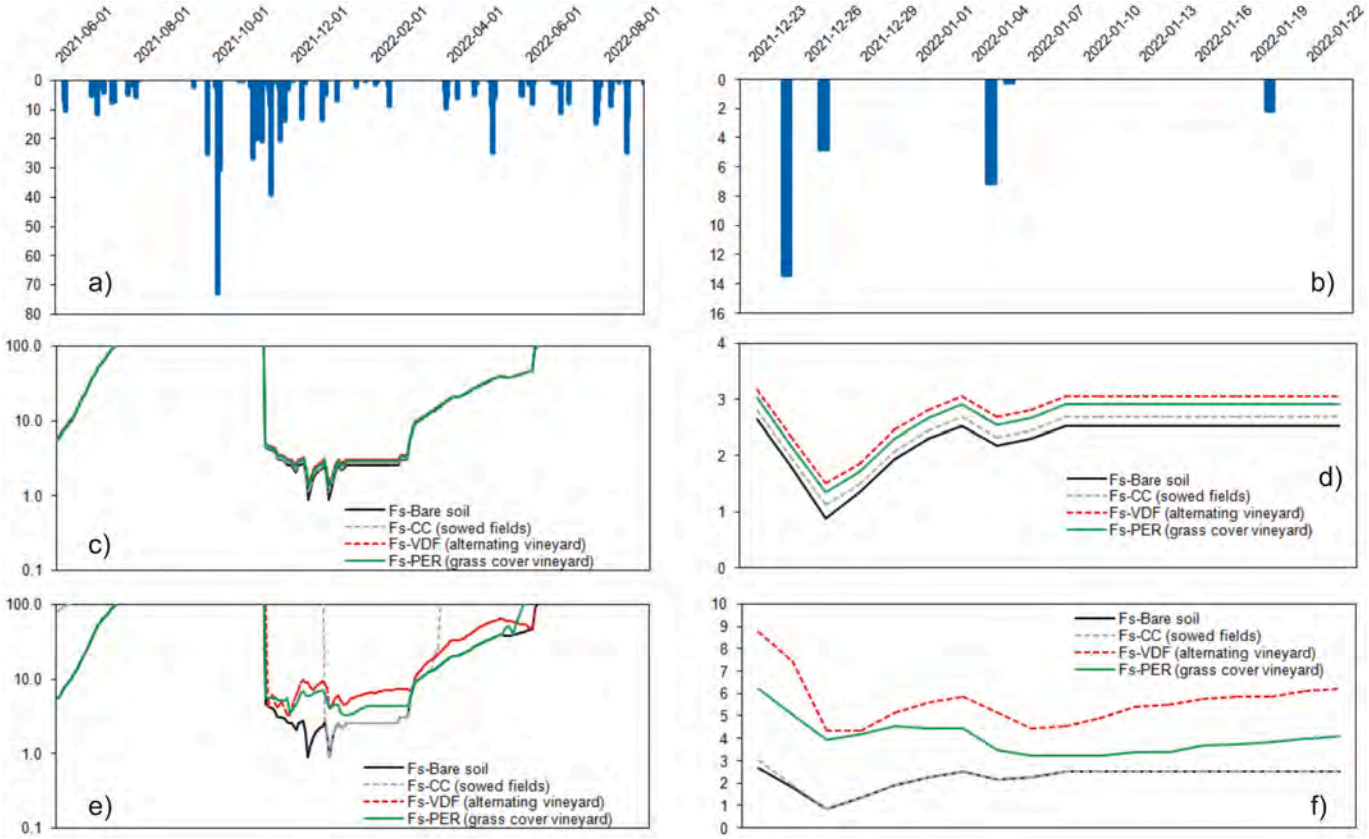

Fig. 12. Trend of calculated daily slope safety factor (Fs) of different land uses considering the role of the different types of root reinforcements: a) rainfall amounts between 1 June 2021 and 31 August 2022; b) rainfall amounts between 23 December 2021 and 23 January 2022; c) Fs calculated considering root mechanical reinforcement between 1 June 2021 and 31 August 2022; d) Fs calculated considering mechanical root reinforcement between 23 December 2021 and 23 January 2022; e) Fs calculated considering root hydrological reinforcement between 1 June 2021 and 31 August 2022; f) Fs calculated considering mechanical root reinforcement between 23 December 2021 and 23 January 2022.

4. Discussion

Vegetation plays a fundamental role in slope stability, particularly in the topmost layers of soil, where the majority ofroots are concentrated. In this context, the selection of optimal vegetation types can serve as a nature-based solution to mitigate the susceptibility of a region to shallow slope instabilities, such as shallow landslides (Gonzalez-Ollauri, 2022; Mao, 2022). This aspect is crucial, even in the case of vulnerable hillslopes that are cultivated with various crops and agricultural practices, to identify the most effective management strategies for reducing the occurrence of slope failures and their associated damages (Wu, 2012).

The selected study area serves as a compelling example of the positive impact that agricultural practices can have on agroecosystems, specifically on hillslopes cultivated with vineyards and sowed fields in the northern Italian Apennines. The assessment of mechanical and hydrological effects induced by different land uses on slope stability, conducted in this study, provides valuable insights applicable to various agroecosystems, whether they share similar or dissimilar land uses. Furthermore, this research contributes to the evaluation of the impacts of other agricultural practices, such as intense tillage and mulching (Gatti et al., 2022), or different cultivated crops, such as orchards and olive yards (De Melo and Van Lier, 2021), on RWU and the stability of steep slopes.

The mechanical influence of vegetation on soil stability near the base of slopes is primarily concentrated within the rooting zone. In this zone, the shallow soil, permeated with roots, functions as a composite material where stresses are distributed between the solid skeleton and the root network (Capobianco et al., 2021). As previously noted by Bordoni et al. (2020), the level of mechanical root reinforcement increases with a higher concentration of roots in the soil layers for the land uses under examination. In this context, it is observed that for the specific land uses in Oltrepò Pavese, the absolute values of c_r range from 12 % to 73 %, which are lower than those reported by Bordoni et al. (2020). Furthermore, the results of this study continue to underscore that grapevines provide a greater mechanical reinforcement compared to sowed fields, particularly in areas with alternating vineyards, extending to depths of up to 1.5 m from ground level.

Sowed areas are characterized by having >80 % of their roots classified as fine, with a diameter of <2 mm. It is worth noting that fine roots provide a lesser contribution to root reinforcement when compared to larger-diameter roots, which are more prevalent in grapevines, constituting over 45 % of the root composition with a diameter exceeding 2 mm (Vergani et al., 2017; Dazio et al., 2018). Among the various agricultural practices employed in vineyards, the development of larger roots in alternating vineyards may be attributed to the presence of a higher quantity of organic matter in the soil profile. This increase is a result of trenching and tillage activities carried out in previously covered interrows. These practices facilitate the movement of a greater quantity of nutrients, thereby promoting further growth in the root system architecture (Costantini et al., 2015).

In the rooting zone, vegetation's hydrological impact on stability arises from processes like evapotranspiration and water uptake, which are essential for plant physiology. These processes lead to a decrease in soil water content and, consequently, a reduction in soil pore water pressure (Terwilliger, 1990). Root mechanical reinforcement can be considered relatively stable over limited periods, especially for cultivated plants like grapevines, as it typically takes >3–5 years to observe a noticeable effect on root density due to changes in agricultural practices or the types of cultivated plants (Smart et al., 2006). In contrast, the hydrological reinforcement effect provided by roots experiences more pronounced fluctuations, including seasonal variations, owing to the occurrence and intensity of water uptake required for plant physiology (Liu et al., 2021).

The trends in saturation degree and pore water pressure, both monitored and modelled within the examined land uses, confirm variations in ch_r across different seasons, even for cultivated plants. This observation aligns with findings in other woody plants (Liu et al., 2021; Boldrin et al., 2021) and shrubs (Ng et al., 2020). The highest ch_r values are observed during the summer season when plant transpiration is at its peak. This period is characterized by prolonged dry and hot days. Conversely, ch_r experiences a continuous and significant decrease during the autumn and winter seasons, when plant transpiration is minimal or absent, coinciding with the coldest and wettest days. There is a ch_r recovery in the spring months, typically starting in March, attributable to changing environmental conditions (Liu et al., 2021).

In addition to the overall pattern observed in both sowed areas and vineyards, it isimportant to note that ch_r varies among the different land uses during specific periods. During the summer months, characterized by dry and hot conditions, all the examined land uses exhibited very low levels of soil water content and pore water pressure. Consequently, ch_r values exceeded 10^2 kPa across all soil depths. However, it was observed that ch_r decreased to around 10^1kPa in all the land uses during October and November. Significant distinctions emerge during late autumn (November), the winter months, and the early spring period (up to May). During this time frame, the soil tends to approach or reach complete saturation, and RWU is minimal or nonexistent due to plant dormancy. During particularly rainy periods, pore water pressure can drop to zero or even become positive within the typical soil layer, where shallow landslides could potentially occur in the study area (1 m from ground level). This situation poses a risk of triggering shallow slope failures. In this specific time interval, notably in December and January, ch_rvalues in sowed fields become zero, while in vineyards, they remain positive, decreasing to at least 0.2 kPa. On average, ch_r values hover around 1.5 kPa in grass-covered vineyards and around 2.8 kPa in alternating vineyards across all the analyzed soil layers.

These results indicate that the water uptake processes by grapevine roots can occur, albeit in a limited capacity, even during the coldest periods of the year and under various agricultural management practices. This observation aligns with the findings of Strack and Stoll (2022). Despite grapevines being deciduous plants, evapotranspiration remains minimal in the autumn and winter months due to the low physiological activity of the plants during dormancy (Allen et al., 1998; Wilson et al., 2020). In contrast, wheat and alfalfa, which are present in the studied sowed areas, exhibit negligible water uptake after being mowed and harvested at the end of summer and the beginning of autumn (Penna et al., 2020). During these months, the measured ch_rvalues in alternating vineyards are higher than those in vineyards covered with grass. This difference can be attributed to variations in root density, as a more developed root system in the soil profile leads to greater water uptake (Boldrin et al., 2021). Indeed, the root density of the tested alternating vineyards, assessed using the Root Area Ratio (RAR) index (Bischetti et al., 2009), is, on average, 25 % higher in alternating vineyards compared to those covered with grass throughout the entire soil profile. Specifically, root densities are measured at 0.104 % in alternating vineyards and 0.078 % in grass-covered vineyards, with differences ranging from 15 % to 39 % across various soil layers.

Distinct trends in ch_r were observed during the early spring months (March to May). In sowed fields, ch_r values began to rise earlier than in vineyards, transitioning from 10^1 kPa to levels exceeding 10^3 kPa within a span of 28 to 30 days. Conversely, ch_r remained below 10 kPa in vineyards with permanent grass cover until the first half of May and in alternating vineyards until the beginning of June. These variations may be attributed to differences in the timing of the most active physiological processes between these plants. It appears that these processes are initiated earlier in sowed fields with crops like wheat and alfalfa compared to grapevines. The disparities among the various types of vineyards can be attributed to the presence of spontaneous grasses in the interrows of grass-covered vineyards, characterized by a typical RAR of 0.021 % within the first 0.2 m from the ground level. These grasses tend to flourish during the spring months, leading to additional evapotranspiration from the soil layers (Bogunovic et al., 2019).

The contrasting behaviours of mechanical and hydrological reinforcements have a significant impact on shallow slope stability. This is evident from the modelled trends of Fs reconstructed when considering bare soils (no reinforcement), solely mechanical reinforcement, and exclusively the hydrological reinforcement effect, respectively. When focusing solely on mechanical reinforcement, the increment in Fs attributed to plant roots remains within a range of 7 %, displaying relative stability across various soil hydrological conditions. Notably, grapevines' mechanical reinforcement provides a more substantial increase in Fs (ranging from 5.1 % to 7.2 %) compared to sowed fields (with increases ranging from 2.2 % to 2.7 %). This observation aligns with the higher root density of grapevines, which results in a greater contribution in terms of c_r(as confirmed by Bordoni et al., 2020).

Conversely, the hydrological reinforcement effect exhibits variations across different seasons, primarily influenced by the amount of water extracted through plant activities and evapotranspiration, leading to corresponding changes in pore water pressure (Simon and Collison, 2002). Previous research on the hydrological effects of roots on soil hydrological trends and slope stability was conducted in various climatic contexts and involving different woody plants and shrubs (Comegna et al., 2013; Gonzalez-Ollauri and Mickovski, 2017; Capobianco et al., 2021; Liu et al., 2021), has consistently demonstrated that vegetation exerts its most significant hydrological reinforcement effect during dry and hot seasons (exceeding 60 % in sowed fields and over 70 % in vineyards). This pattern was similarly observed in the study area during the period between May and October. Regarding the c_r effect, grapevine plants are capable of providing a more substantial increase in Fs through hydrological reinforcement compared to sowed fields, thanks to their higher root density and consequent water uptake capacity.

Nevertheless, grapevine plants demonstrate their capacity to extract a sufficient amount of water even during the cold and wet seasons of the year, spanning from November to April. This period coincides with the increased likelihood of triggering shallow landslides due to saturated soil conditions (Bordoni et al., 2021). During this season, the influence of ch_r becomes evident, leading to significant increases in Fs. In vineyards managed with alternating methods and permanent grass cover, Fs can surge by 3.5 times (350 %) and two times (226 %), respectively, compared to bare soil conditions. In contrast, in sowed areas, the ch_r-driven increase averages only 5 % during the same wet season. However, it can become negligible during extremely intense rainfall events, as observed during the monitoring period (e.g., 18.2 mm of rainfall in 2 days on 25–27 December 2022). These differences are particularly significant, especially during periods when rainfall events can lead to an additional increase in pore water pressure, reaching positive values of up to 1.4 kPa. This increase in pore water pressure results in a decrease in Fs (as shown in Fig. 11d, f). In particular, focusing on the period 23 December 2021–23 January 2022, a rainfall event caused a substantial decrease in Fs. However, the presence of c_r helped maintain Fs values above 1, ranging from 1.2 to 1.9, for all the analyzed agroecosystems. In contrast, Fs dropped below 1, indicating unstable conditions for bare soils during these rainy days.Instead, when considering the effect of ch_r, Fs values remained significantly higher than 1, ranging from 3.2 to 7.4, in vineyards. However, Fs values for sowed fields decreased below 1 when the root hydrological reinforcement in this land use became negligible, following a trend similar to that observed in bare soil.

These results affirm the beneficial impact of root reinforcement from various plants and agricultural practices that are characteristic of typical agroecosystems in a broad region such as Oltrepò Pavese in the Italian Apennines. For the land uses examined, both the mechanical and hydrological reinforcement effects contribute to enhancing shallow slope stability compared to vegetation-free soils for most of the seasons throughout the year. In addition to the positive effects of these reinforcements, the presence of dying or decaying roots within a soil profile could potentially have adverse impacts on shallow slope stability. This is because it can lead to the development of preferential flow paths, which may increase soil permeability and limit the ability of vegetated hillslopes to reduce soil water content and pore water pressure within the upper meters of the soil profile (Ghestem et al., 2011; Ni et al., 2018). Moreover, within the same land use, the variability of hydrological reinforcement effects, due to particular meterological conditions, peculiar site-specific land use distribution (Capobianco et al., 2021) or geological and geomorphological settings (Boldrin et al., 2021), could provoke local increase in soil water content and pore water pressure. This could reduce or cancel the differences in terms of hydrological reinforcement between land uses induced by their root water uptakes.

Neglecting these conditions, the stabilizing contribution of mechanical reinforcement is on average higher than the hydrological reinforcement effect and can guarantee an increase of slope stability also in wet periods, when shallow landslides can develop more frequently (Liu et al., 2021). Hydrological reinforcement effect induced by processes of plant–water uptake from soil could contribute to slope stability more than the mechanical one in dry periods. During the cold and wet season, the variability of hydrological reinforcement effect appeared very high. Thus, hydrological root reinforcement could give a contribution to slope stability in agreement with the one of the mechanical reinforcement when a plant, as the analyzed grapevines, is able to uptake sufficient rates of water to reduce significantly pore water pressure, guaranteeing values of hydrological reinforcement effect on average around 1–3 kPa.

Besides these low values, these measures are significant since they are above the typical accuracy of the field instruments used for pore water pressure monitoring in conditions close to saturation (tensiometers, accuracy around 0.5 kPa). Moreover, as shown in the performed slope stability analyses, these values of hydrological reinforcement are enough to keep slope Fs slightly higher than 1, guaranteeing stable conditions also when bare soils, which cannot experience this effect, could become unstable in correspondence of particular rainfall events.

The analyses carried out in this study tried to estimate the role of mechanical and hydrolgical reinforcementas separated effects. However, these two processes can act together in a soil profile (Capobianco et al., 2021; Gonzalez-Ollauri, 2022; Mao, 2022), allowing a further increase of shallow slope stability.

5. Conclusions

The paper presented comparison analyses between root mechanical and hydrological reinforcement effects on shallow slope stability in some typical agroecosystems in northern Italy, such as sowed fields and vineyards with different interrows management. Considering the same meterological setting, land use type has a significant effect on saturation degree and pore water pressure trends, due to the different ability of roots to uptake water from soils. This has a direct effect on the hydrological reinforcement provided by these land uses. For all the tested sites, root hydrological reinforcement effect due to transpiration and drying of soils is higher in summer, with values of 1–2 order of magnitude higher than the root mechanical reinforcement. In wet and cold periods, when shallow landslides can develop more frequently, the stabilizing contribution of mechanical reinforcement is on average higher than the hydrological reinforcement effect and can guarantee an increase in shallow slope stability. However, in vineyards, the hydrological reinforcement effect could be observed also during wet winter periods, although evapotranspiration is minimal. For these reasons, the hydrological reinforcement effect provided in grapevines during wet and cold periods could give a contribution to slope stability in agreement with the mechanical reinforcement effect. This situation occurs when plants are able to uptake enough water from soil to reduce significantly pore water pressure, guaranteeing values of hydrological reinforcement effect in the range of 1–3 kPa.

These results suggest that in the assessment of susceptibility towards shallow landslides both mechanical and hydrological effects of vegetation deserve high regard. These analyses could also indicate which best agricultural practices and land uses could be implemented in land

planning to reduce the probability of occurrence of these failures over large cultivated territories. Furthermore, these results could be included on additional simulations, through slope stability models, for analysing the effects of vegetation in correspondence of extreme rainfall intensities and future scenarios of climate change.

CRediT authorship contribution statement

Massimiliano Bordoni: Conceptualization, Data curation, Formal analysis, Investigation, Methodology, Validation, Writing – original draft, Writing – review & editing. **Valerio Vivaldi:** Data curation, Formal analysis, Investigation, Methodology, Writing – review & editing. **Alessia Giarola:** Formal analysis, Investigation, Writing – review & editing. **Roberto Valentino:** Validation, Writing – review & editing. **Marco Bittelli:** Validation, Writing – review & editing. **Claudia Meisina:** Data curation, Investigation, Methodology, Supervision, Writing – review & editing.

Declaration of competing interest

The authors declare that they have no known competing financial interests or personal relationships that could have appeared to influence the work reported in this paper.

Data availability

Data will be made available on request.

Acknowledgements

This work has been in the frame of the VIRECLI project, which has been supported by Regione Lombardia. Moreover, we thank the companies that allowed to make the field surveys in vineyards: Azienda Ferrari, Azienda Conte Vistarino. We thank the Anonymous Reviewers for their revisions and suggestions to the work.

References

Allen, R.G., Pereira, L.S., Raes, D., Smith, M., 1998. Crop evapotranspiration: guidelines for computing crop water requirements. In: FAO Irrigation and Drainage Paper No. 56. FAO, Rome.

Arnaez, J., Lasanta, T., Errea, M., Ortigosa, L.M., 2011. Land abandonment, landscape evolution, and soil erosion in a Spanish Mediterranean mountain region: the case of Camero Viejo. Land Degrad. Dev. 22 (6), 537–550.

Baum, R.L., Savage, W.Z., Godt, J.W., 2008. TRIGRS – A FORTRAN Program for Transient Rainfall Infiltration and Grid-Based Regional Slope-Stability Analysis, Version 2.0: US Geological Survey Open-File Report 2008-1159 (81 pp.).

Bischetti, G.B., Chiaradia, E.A., Epis, T., Morlotti, E., 2009. Root cohesion of forest species in the Italian Alps. Plant Soil 324, 71–89.

Bogunovic, I., Andabaka, Z., Stupic, D., Pereira, P., Galic, M., Novak, K., Telak, L.J., 2019. Continuous grass coverage as a management practice in humid environment vineyards increases compaction and CO2 emissions but does not modify must quality. Land Degrad. Dev. 30, 2347–2359.

Bohm, W., 1979. Methods of Studying Root Systems. Ecological Studies. Springer, Berlin, (Germany), p. 33.

Boldrin, D., Leung, A.K., Bengough, A., 2018. Hydrologic reinforcement induced by contrasting woody species during summer and winter. Plant Soil 427, 369–390.

Boldrin, D., Leung, A.K., Bengough, A., 2021. Hydro-mechanical reinforcement of contrasting woody species: a full-scale investigation of a field slope. Geotechnique 71 (11), 970–984.

Bordoloi, S., Ng, C.W.W., 2020. The effects of vegetation traits and their stability functions in bio-engineered slopes: a perspective review. Eng. Geol. 275, 105742 https://doi.org/10.1016/j.enggeo.2020.105742.

Bordoni, M., Meisina, C., Vercesi, A., Bischetti, G.B., Chiaradia, E.A., Vergani, C., Chersich, S., Valentino, R., Bittelli, M., Comolli, R., Persichillo, M.G., Cislaghi, A., 2016. Quantifying the contribution of grapevine roots to soil mechanical reinforcement in an area susceptible to shallow landslides. Soil Tillage Res. 163, 195–206.

Bordoni, M., Vercesi, A., Maerker, M., Ganimede, C., Reguzzi, M.C., Capelli, E., Wei, X., Mazzoni, E., Simoni, S., Gagnarli, E., Meisina, C., 2019. Effects of vineyard soil management on the characteristics of soils and roots in the lower Oltrepò Apennines (Lombardy, Italy). Sci. Total Environ. 693, 133390 https://doi.org/10.1016/j.scitotenv.2019.07.196.

Bordoni, M., Cislaghi, A., Vercesi, A., Bischetti, G.B., Meisina, C., 2020. Effects of plant roots on soil shear strength and shallow landslide proneness in an area of northern Italian Apennines. Bull. Eng. Geol. Environ. https://doi.org/10.1007/s10064-020-01783-1.

Bordoni, M., Bittelli, M., Valentino, R., Vivaldi, V., Meisina, C., 2021. Observations on soil-atmosphere interactions after long-term monitoring at two sample sites subjected to shallow landslides. Bull. Eng. Geol. Environ. 80, 7467–7491.

Brambilla, M., Casale, F., Bergero, V., Bogliani, G., Crovetto, G.M., Falco, R., Roati, M., Negri, I., 2010. Glorious past, uncertain present, bad future? Assessing effects of land-use changes on habitat suitability for a threatened farmland bird species. Biodivers. Conserv. 143, 2770–2778.

Cammeraat, E., Beek, R., Kooijman, A., 2005. Vegetation succession and its consequences for slope stability in SE Spain. Plant Soil 278 (1–2), 135–147.

Capobianco, V., Robinson, K., Kalsnes, B., Ekeheien, C., Høydal, Ø., 2021. Hydro-mechanical effects of several riparian vegetation combinations on the streambank stability—a benchmark case in Southeastern Norway. Sustainability 13, 4046. https://doi.org/10.3390/su13074046.

Cevasco, A., Pepe, G., Brandolini, P., 2014. The influences of geological and land use settings on shallow landslides triggered by an intense rainfall event in a coastal terraced environment. Bull. Eng. Geol. Environ. 73, 859–875.

Chen, J., Lei, X.-W., Zhang, H.-L., Lin, Z., Wang, H., Hu, W., 2021. Laboratory model test study of the hydrological effect on granite residual soil slopes considering different vegetation types. Sci. Report. 11, 14668. https://doi.org/10.1038/s41598-021-94276-4.

Ciurleo, M., Calvello, M., Cascini, L., 2016. Susceptibility zoning of shallow landslides in fine grained soils by statistical methods. Catena 139, 250–264.

Cohen, D., Schwarz, M., 2017. Tree-root control of shallow landslides. Earth Surf. Dynam. 5, 451–477.

Comegna, L., Damiano, E., Greco, R., Guida, A., Olivares, L., Picarelli, L., 2013. Effects of the vegetation on the hydrological behavior of a loose pyroclastic deposit. Procedia Environ. Sci. 19, 922–931.

Costantini, E.A.C., Agnelli, A.E., Fabiani, A., Gagnarli, E., Mocali, S., Priori, S., Simoni, S., Valboa, G., 2015. Short-term recovery of soil physical, chemical, micro and meso biological functions in a new vineyard under organic farming. Soil 1, 443–457.

Cruden, D.M., Varnes, D.J., 1996. Landslide types and processes. In: Turner, A.K., Schuster, R.L. (Eds.), Landslides: Investigation and Mitigation Sp. Rep, 247. Transportation Research Board, National Research Council, National Academy Press, Washington DC, pp. 36–75.

Dazio, E., Conedera, M., Schwarz, M., 2018. Impact of different chestnut coppice managements on root reinforcement and shallow landslide susceptibility. For. Ecol. Manag. 417, 63–76.

De Melo, M.L.A., Van Lier, Q.J., 2021. Revisiting the Feddes reduction function for modeling root water uptake and crop transpiration. J. Hydrol. 603B, 126952 https://doi.org/10.1016/j.jhydrol.2021.126952.

Feddes, R.A., Kowalik, P.J., Zaradny, H., 1978. Simulation of Field Water Use and Crop Yield. Centre for agricultural publishing and documentation, Wageningen.

Fredlund, D.G., Morgenstern, N.R., Widger, R.A., 1978. The shear strength of unsaturated soils. Can. Geotech. J. 15 (3), 313–321.

Froude, M.J., Petley, D.N., 2018. Global fatal landslide occurrence from 2004 to 2016. Nat. Hazards Earth Syst. Sci. 18, 2161–2181.

Gariano, S.L., Petrucci, O., Rianna, G., Santini, M., Guzzetti, F., 2018. Impacts of past and future land changes on landslides in southern Italy. Reg. Environ. Chang. 18 (437), 449.

Gatti, M., Garavani, A., Squeri, C., Diti, I., De Monte, A., Scotti, C., Poni, S., 2022. Effects of intra-vineyard variability and soil heterogeneity on vine performance, dry matter and nutrient partitioning. Precis. Agric. 23, 150–177.

Ghestem, M., Sidle, R.C., Stokes, A., 2011. The influence of plant root systems on subsurface flow: implications for slope stability. BioScience 61, 869–879.

Giannecchini, R., Galanti, Y., D'Amato Avanzi, G., 2012. Critical rainfall thresholds for triggering shallow landslides in the Serchio River Valley (Tuscany, Italy). Nat. Hazards Earth Syst. Sci. 12, 829–842.

Gonzalez-Ollauri, A., 2022. Sustainable use of nature-based solutions for slope protection and erosion control. Sustainability 14, 1981. https://doi.org/10.3390/su14041981.

Gonzalez-Ollauri, A., Mickovski, S.B., 2017. Hydrological effect of vegetation against rainfall-induced landslides. J. Hydrol. 549, 374–387.

Grelle, G., Soriano, M., Revellino, P., Guerriero, L., Anderson, M.G., Diambra, A., Fiorillo, F., Esposito, L., Diodato, N., Guadagno, F.M., 2014. Space–Time Prediction of Rainfall-induced Shallow Landslides Through a Combined Probabilistic/Deterministic Approach, Optimized for Initial Water Table Conditions. Bull. Eng. Geol, Environ.

IPCC, 2022. In: Pörtner, H.-O., Roberts, D.C., Tignor, M., Poloczanska, E.S., Mintenbeck, K., Alegría, A., Craig, M., Langsdorf, S., Löschke, S., Möller, V., Okem, A., Rama, B. (Eds.), IPCC, 2022: Climate Change 2022: Impacts, Adaptation and Vulnerability. Contribution of Working Group II to the Sixth Assessment Report of the Intergovernmental Panel on Climate Change. Cambridge University Press, Cambridge University Press, Cambridge, UK and New York, NY, USA. https://doi.org/10.1017/9781009325844, 3056 pp.

de Jesus Arce-Mojica, T., Nehren, U., Sudmeier-Rieux, K., Miranda, P.J., Anhuf, D., 2019. Nature-based solutions (NbS) for reducing the risk of shallow landslides: where do we stand? Int. J. Dis. Risk Red. 41, 101293 https://doi.org/10.1016/j.ijdrr.2019.101293.

Krause, P., Boyle, D.P., Bäse, F., 2005. Comparison of different efficiency criteria for hydrological model assessment. Adv. Geosci. 5, 89–97.

Lesschen, J.P., Cammeraat, L.H., Nieman, T., 2008. Erosion and terrace failure due to agricultural land abandonment in a semi-arid environment. Earth Surf. Process. Landf. 1584, 1574–1584.

Leung, A.K., Boldrin, D., Liang, T., Wu, Z.Y., Kamchoom, V., Bengough, A., 2018. Plant age effects on soil infiltration rate during early plant establishment. Géotechnique 68 (7), 646–652.
Levia, D.F., Germer, S., 2015. A review of stemflow generation dynamics and stemflow–environment interactions in forests and shrublands. Rev. Geophys. 53 (3), 673–714.
Liu, H., Mao, Z., Wang, Y., Kim, J.H., Bourrier, F., Mohamed, A., Stokes, A., 2021. Slow recovery from soil disturbance increases susceptibility of high elevation forests to landslides. For. Ecol. Manag. 485, 118891 https://doi.org/10.1016/j.foreco.2020.118891.
Lu, J., Zhang, Q., Werner, A.D., Li, Y., Jiang, S., Tan, Z., 2020. Root-induced changes of soil hydraulic properties – a review. J. Hydrol. 589, 125203 https://doi.org/10.1016/j.jhydrol.2020.125203.
Mao, Z., 2022. Root reinforcement models: classification, criticism and perspectives. Plant Soil 472, 17–28.
Masi, E.B., Segoni, S., Tofani, V., 2021. Root reinforcement in slope stability models: a review. J. Geosci. 11, 212. https://doi.org/10.3390/geosciences11050212.
Montrasio, L., Valentino, R., 2008. A model for triggering mechanisms of shallow landslides. Nat. Hazards Earth Syst. Sci. 8, 1149–1159.
Moos, C., Bebi, P., Schwarz, M., Stoffel, M., Sudmeier-Rieux, K., Dorren, L., 2018. Ecosystem based disaster risk reduction in mountains. Earth Sci. Rev. 177, 497–513.
Morgan, R.P.C., Rickson, R.J., 2003. Slope Stabilization and erosion Control: A Bioengineering Approach. Taylor & Francis.
Nash, J.E., Sutcliffe, J.V., 1970. River flow forecasting through conceptual models - part I: a discussion of principles. J. Hydrol. 10, 282–290.
Ng, C.W.W., Ni, J.J., Leung, A.K., 2020. Effects of plant growth and spacing on soil hydrological changes: a field study. Geotechnique 70 (10), 867–881.
Ng, C.W.W., Zhang, Q., Chao, Z., Ni, J.J., 2022. Eco-geotechnics for human sustainability. Sci. China Technol. Sci. 65 https://doi.org/10.1007/s11431-022-2174-9.
Ni, J.J., Leung, A.K., Ng, C.W.W., Shao, W., 2018. Modelling hydro-mechanical reinforcements of plants to slope stability. Comput. Geotech. 95, 99–109.
Ni, J.J., Cheng, Y., Wang, Q., Ng, C.W.W., Garg, A., 2019. Effects of vegetation on soil temperature and water content: field monitoring and numerical modelling. J. Hydrol. 571, 494–502.
Panagos, P., Ballabio, C., Himics, M., Scarpa, S., Matthews, F., Bogonos, M., Poesen, J., Borrelli, P., 2021. Projections of soil loss by water erosion in Europe by 2050. Environ. Sci. Pol. 124, 380–392.
Penna, D., Geris, J., Hopp, L., Scandellari, F., 2020. Water sources for root water uptake: using stable isotopes of hydrogen and oxygen as a research tool in agricultural and agroforestry systems. Agric. Ecosyst. Environ. 291, 106790 https://doi.org/10.1016/j.agee.2019.106790.
Person, G., 1995. Willow stand evapotranspiration simulated for Swedish soils. Agric. Water Manag. 28, 271–293.
Peters, A., Durner, W., 2008. Simplified evaporation method for determining soil hydraulic properties. J. Hydrol. 356, 147–162.
Potapov, P., Turubanova, S., Hansen, M.C., Tyukavina, A., Zalles, V., Khan, A., Song, X.-P., Pickens, A., Shen, Q., Cortez, J., 2022. Global maps of cropland extent and change show accelerated cropland expansion in the twenty-first century. Nat. Food 3, 19–28.
Raggi, M., Viaggi, D., Bartolini, F., Furlan, A., 2015. The role of policy priorities and target in the spatial location of participation in agrienvironmental schemes in Emilia-Romagna (Italy). Land Use Policy 47, 78–89.
Rodriguez-Iturbe, I., Porporato, A., 2004. Ecohydrology of Water-controlled Ecosystems. Cambridge University Press, New York, US.
Rossi, R., Picuno, P., Fagnano, M., Amato, M., 2022. Soil reinforcement potential of cultivated cardoon (Cynaracardunculus L.): first data of root tensile strength and density. Catena 211, 106016. https://doi.org/10.1016/j.catena.2022.106016.
Salciarini, D., Fanelli, G., Tamagnini, C., 2017. A probabilistic model for rainfall—induced shallow landslide prediction at the regional scale. Landslides 14, 1731–1746.
Schmidt, K.M., Roering, J.J., Stock, J.D., Dietrich, W.E., Montgomery, D.R., Schaub, T., 2001. The variability of root cohesion as an influence on shallow landslide susceptibility in the Oregon Coast Range. Can. Geotech. J. 38, 995–1024.
Schwarz, M., Giadrossich, F., Cohen, D., 2013. Modeling root reinforcement using a root failure Weibull survival function. Hydrol. Earth Syst. Sci. 17, 4367–4377.
Simon, A., Collison, A.J.C., 2002. Quantifying the mechanical and hydrologic effects of riparian vegetation on streambank stability. Earth Surf. Process. Landf. 27, 527–546.
Simunek, J., Van Genuchten, M.T., Sejna, M., 2012. Hydrus: model use, calibration, and validation. Trans. ASABE 55, 1261–1274.
Smart, D.R., Schwass, E., Lakso, A., Morano, L., 2006. Grapevine rooting patterns: a comprehensive analysis and a review. Am. J. Enol. Vitic. 57 (1), 89–104.
Stokes, A., Douglas, G.B., Fourcaud, T., Giadrossich, F., Gillies, C., Hubble, T., Kim, J.H., Loades, K.W., Mao, Z., McIvor, I.R., Mickovski, S.B., Mitchell, S., Osman, N., Phillips, C., Poesen, J., Polster, D., Preti, F., Raymond, P., Rey, F., Schwarz, M., Walker, L.R., 2014. Ecological mitigation of hillslope instability: ten key issues facing researchers and practitioners. Plant Soil 377 (1–2), 1–23.
Strack, T., Stoll, M., 2022. Soil water dynamics and drought stress response of Vitisvinifera L. in steep slope vineyard systems. Agricul. Water Manag. 274, 107967. Surf. Proces.Landforms 15, 553–570. https://doi.org/10.1016/j.agwat.2022.107967.
Tarolli, P., 2018. Agricultural terraces special issue preface. Land Degrad. Dev. 29, 3544–3548.
Tarolli, P., Straffelini, E., 2020. Agriculture in hilly and mountainous landscapes: threats, monitoring and sustainable management. Geograp. Sust. 1, 70–76.
Tarolli, P., Pijl, A., Cucchiaro, S., Wei, W., 2021. Slope instabilities in steep cultivation systems: process classification and opportunities from remote sensing. Land Degrad. Dev. 32 (3), 1368–1388.
Taylor, S.A., Ashcroft, G.L., 1972. Physical Edaphology: The Physics of Irrigated and Nonirrigated Soils. Freeman, W.H.
Terwilliger, V.J., 1990. Effects of vegetation on soil slippage by pore pressure modification. Earth Surf. Process. Landforms 15 (6), 553–570.
Van Genuchten, M.T., 1980. A closed-form equation for predicting the hydraulic conductivity of unsaturated soils. Soil Sci. Soc. Am. J. 44, 892–898.
Vergani, C., Graf, F., 2016. Soil permeability, aggregate stability and root growth: a pot experiment from a soil bioengineering perspective. Ecohydrology 9 (5), 830–842.
Vergani, C., Werlen, M., Conedera, M., Cohen, D., Schwarz, M., 2017. Investigation of root reinforcement decay after a forest fire in a Scots pine (Pinussylvestris) protection forest. For. Ecol. Manag. 400, 339–352.
Veylon, G., Ghestem, M., Stokes, A., Bernard, A., 2015. Quantification of mechanical and hydric components of soil reinforcement by plant roots. Can. Geotech. J. 52, 1839–1849.
Wesseling, J.G., Elbers, J.A., Kabat, P., Van den Broek, B.J., 1991. SWATRE: Instructions for Input. Internal Note, Winand Staring Centre, Wageningen, the Netherlands.
Wilson, T.G., Kustas, W.P., Alfieri, J.G., Anderson, M.C., Gao, F., Prueger, J.H., McKee, L. G., Mar Alsina, M., Sanchez, L.A., Alstad, K.P., 2020. Relationships between soil water content, evapotranspiration, and irrigation measurements in a California drip-irrigated Pinot noir vineyard. Agric. Water Manag. 237, 106186 https://doi.org/10.1016/j.agwat.2020.106186.
Wu, T.H., 2012. Root reinforcement of soil: review of analytical models, test results and application to design. Can. Geotech. J. 50, 259–274.
Yildiz, A., Graf, F., Rickli, C., Springman, S.M., 2019. Assessment of plant-induced suction and its effects on the shear strength of rooted soils. Geotech. Eng. Proc. Inst. Civ. Eng. Geotechn. Eng. 172 (6), 507–519.
Zhu, J., Mao, Z., Wang, Y., Wang, Y., Li, T., Wang, K., Langendoen, E.J., Zheng, B., 2022. Soil moisture and hysteresis affect both magnitude and efficiency of root reinforcement. Catena 219, 106574. https://doi.org/10.1016/j.catena.2022.106574.